Pergamon

Int. J. Multiphase Flow Vol. 23, No. 4, pp. 765–796, 1997

Printed in Great Britain
PII: S0301-9322(97)00017-7
0301-9322/97 $17.00 + 0.00

NUMERICAL SIMULATION OF A TWO-PHASE TURBULENT PIPE-JET FLOW LOADED WITH POLYDISPERSED SOLID ADMIXTURE

F. FRISHMAN, M. HUSSAINOV, A. KARTUSHINSKY† and A. MULGI
Department of Aeromechanics, Institute of Energy Research, Estonian Academy of Sciences, Paldiski Rd 1, EE0001 Tallinn, Estonia

(Received 22 August 1996; in revised form 13 February 1997)

Abstract—Results of the mathematical modelling of a two-phase turbulent pipe-jet flow carrying fine solid particles are presented. The numerical results are compared with experimental data obtained in our laboratory. The purpose of the joint study of these flows is connected with the efforts to explain the pinch-effect experimentally discovered by Laats and Frishman (1970) and Navoznov *et al.* (1979) (for the motion of fine solid particles in a jet). It is associated with the growth of particle mass concentration along the jet axis with its maximum at some distance from the outlet of the pipe. The effect of intensive scattering of large particles in the initial region of the two-phase turbulent jet was also discovered in those experimental investigations. The theoretical analysis made by Kartushinsky (1984) showed that these effects are linked not only with the properties of the motion of particles of different size in the turbulent jet, but also with the prehistory of the motion of such particles in a pipe.

Our calculations of the pipe-jet flow provide an opportunity to trace the development of the particle mass concentration and the velocity fields in the pipe and jet, excluding the necessity for artificially given initial boundary conditions in the jet for modelling the pinch-effect. The peculiarity of this simulation is in the closure of the equations of the motion of the dispersed phase. The inter-particle collisions in polydispersed flows are considered, since in real two-phase flows the dispersed admixture itself is a polydispersed medium and, thus, the inter-particle collisions play a significant role together with the turbulent diffusion of particles in modelling. The so-called pseudo-viscosity coefficients are introduced in the transport equations of mass, momentum and angular momentum of the dispersed phase for modelling the inter-particle collisions. The formulae for pseudo-viscosity coefficients take into account the properties of the particle motion (the linear and angular velocities and mass concentration of the dispersed phase), their relaxation features as well as collision parameters (the restitution and friction coefficients). The system of equations for the motion of each particle fraction is written and solved for a pipe-jet flow. The exchange of the momentum in the fluctuating motion of the gaseous and dispersed phases is taken into account together with the inter-particle collisions. Such exchange of the momentum results to the additional force factors—the Reynolds stresses in the dispersed phase (Shraiber *et al.* 1990). Besides, the viscous drag force, the Magnus and Saffman lift forces and the turbophoresis force due to the velocity lag as well as non-uniform distribution of the average and the fluctuating velocities of gaseous phase are also taken into account in the model. Only due to the consideration of all these factors it has been possible to simulate the pinch-effect in a two-phase jet. The numerical results are in good agreement with the experimental data for the pipe and jet flow. © 1997 Elsevier Science Ltd.

Key Words: pipe-jet flow, modelling, inter-particle collisions, pinch-effect, turbophoresis force, pseudo-viscosity coefficients

1. INTRODUCTION

An attempt of mathematical describing of the peculiarities of the particle mass concentration in the turbulent motion of fine solid particles in the pipe-jet flow by numerical calculation is presented. The numerical results are compared with the experimental data obtained in our laboratory. The anomalous behaviour of distributions of the particle mass concentration were experimentally found by Laats and Frishman (1970) and Navoznov *et al.* (1979) in a two-phase free round turbulent jet. The pinch-effect is associated with the growth of particle mass concentration along the axis of the jet and observed for the motion of fine solid particles in the initial development stage of the jet. For the motion of large particles, the scattering effect, which is expressed by steep attenuation of the particle mass concentration in the initial stage of the jet development was also

†To whom all correspondence should be addressed.

observed. The experimental investigations showed also the distribution of particle mass concentration with wavy profile along the axis. The particles are scattered in the initial stage of the jet development and concentrated downstream the flow. Far away from the pipe outlet in the fully developed region of the jet, the particles become scattered again due to the turbulent diffusion. The experiments showed that with the increase of the particle size the pinch-effect transformed gradually into the scattering effect. The analysis of the admixture motion in a pipe and jet showed close inter-dependence of both effects—the pinch-effect and the scattering effect due to the motion characteristics resulting from different particle size. So, the scattering effect in a two-phase jet is accompanied by the motion of large solid particles in the pipe with the substantial velocity lag between the gaseous and dispersed phases (Hussainov *et al.* 1996). The pinch-effect can be observed for the motion of fine solid particles with practically zero velocity lag between two phases in the pipe (Laats and Frishman 1970; Navoznov *et al.* 1979). At that time there was practically only one theoretical article where an attempt of explaining these anomalous effects was made. Kartushinsky (1984) showed that for the description of these anomalies the migration process should be included together with the turbulent transport of solid particles in a two-phase turbulent jet. It was assumed that the only reason for the emergence of anomaly was the Magnus force having impact on rotating particles, which moved with a velocity lag. This article demonstrated successfully by numerical calculations that for the definite values of the flow parameters at the outlet of the pipe the experimentally observed anomalies could be described well when neglecting the hypothesis of the velocity equilibrium for gaseous and dispersed phases in the radial direction. At that time such hypothesis was used by many authors (Abramovich *et al.* 1972; Vasilkov 1976; Melville and Bray 1979). The difficulty of the numerical task (Kartushinsky 1984) was stipulated by the lack of necessary information about the angular velocity distribution as well as radial velocity components of the particles at the outlet of the pipe. Such distributions were taken from the numerical results, which were in good agreement with the experimental data. Kartushinsky (1984) came to the conclusion that for the proper modelling of the pinch and scattering effects, calculations of the pipe-jet flow were necessary in order to define the initial boundary conditions for the two-phase turbulent jet correctly, in particular for the angular velocity of particles, which could be neither calculated nor measured at that time. The given calculations of the two-phase turbulent pipe-jet flow allow to trace the development of the flow in the pipe and jet and determine the parameters at the outlet of the pipe as well.

In 1970–1973 several articles (Laats and Frishman 1970; Hetsroni and Sokolov 1971; Laats and Frishman 1973) were published where the effect of the turbulence attenuation by particles was experimentally discovered. These works initiated the elaboration of models describing such influence of the dispersed phase on turbulence. Based on the Prandtl's theory, Abramovich (1970) found a relation for fluctuating velocities of the gaseous phase where the attenuation of the fluctuating velocity of gaseous phase was included. Later, Yarin and Hetsroni (1994a) used the same Prandtl's theory and elaborated a model showing the influence of non-uniform distribution of the dispersed phase composition (bimodal particle composition) on the turbulence of the carrier fluid. It was demonstrated that in such a polydispersed admixture the turbulence intensity might be enhanced as well as attenuated compared to the turbulence intensity of the flow carrying monodispersed admixture, depending on the ratio of the particle size. Using the two-parameter k–ϵ turbulence model, Elghobashi and About-Arab (1983), Shraiber *et al.* (1990) elaborated some closure models for two-phase turbulent flows taking into account two-way coupling. They described the effect of turbulence attenuation by introducing additional terms in the differential transport equations for the turbulent energy and rate of its dissipation originated from the viscous drag force. Yarin and Hetsroni (1994b) suggested a model where the enhancement or attenuation of the turbulence intensity was described not only by one parameter—the correlation of the particle size and scale of turbulence, but additionally by three more parameters—the ratio of particle and gas densities, the particle Reynolds number and mass loading of the flow.

As it can be seen from our experimental investigations in a horizontal pipe, in the fully developed, steady flow the dispersed phase moved with or without the substantial velocity lag between two phases depending on the flow conditions (Navoznov *et al.* 1979). With large particles flowing in the pipe, the velocity lag reached 25% from the velocity of the carrier flow. As our investigations showed, the main parameter, which determined such motion with the velocity lag was the Stokes

number (Hussainov *et al.* 1996). The distribution of particle mass concentration in the cross-section of such two-phase flows with velocity lag is non-uniform with the maximum value at the axis of the pipe (Navoznov *et al.* 1979). When the particles have very small velocity lag, as for example, fine particles, the maximum value of the particle mass concentration in the cross-section is located in the vicinity of the pipe wall. The motion of admixture with velocity lag has also been experimentally observed in vertical pipe flows (Kramer and Depew 1972; Lee and Durst 1982; Tsuji *et al.* 1984) and channel flows (Kulick *et al.* 1994). It should be underlined that the profiles of the particle mass concentration in experiments were close to uniform with the slight increase of concentration towards the wall (Kulick *et al.* 1994).

A great number of articles has been devoted to theoretical studies of two-phase flows in pipes and channels. In general, there are two different approaches to the description of the motion of such two-phase flows—the Lagrange approach (Crowe *et al.* 1977; Sommerfeld 1992; Sommerfeld and Zivkovic 1992) and the Euler approach (Elghobashi and About-Arab 1983; Louge *et al.* 1991; He and Simonin 1993). The main issue in applying the Euler approach is included in the closure of transport equations of the dispersed phase and writing the boundary conditions for these equations. There are no such problems for the Lagrange approach and here the boundary conditions for single particles seem to be more attractive from the physical point of view. Recently, Sommerfeld (1992) found the significant influence of the wall roughness on the particle motion in a channel. However, to take into account two-way coupling for the Lagrange approach a special procedure (Crowe *et al.* 1977) was elaborated. The method was further developed by Kohnen *et al.* (1994).

The Euler approach is also widespread in the simulations of two-phase pipe and channel flows. Louge *et al.* (1991), He and Simonin (1993) simulated the motion in two-phase vertical rising flows. The difference of these studies is in closure of transport equations of the dispersed phase. Louge *et al.* (1991) used the closure of transport equation based on the theory of rapid granular flows (Jenkins and Savage 1983) where the momentum exchange in the dispersed phase was simulated by particle collisions. In this model the closure was considered in the equilibrium approximation where only one transport equation of the dispersed phase (for the so-called 'granular temperature') expressed in terms of the r.m.s. particle velocity fluctuations is applied for the closure, on the contrary to the closure presented by He and Simonin (1993) where the transport equations of the dispersed phase were written for different stress tensor components. In both studies (Louge *et al.* 1991; He and Simonin 1993) the velocity slip of the dispersed phase along the wall was used for writing the boundary conditions.

On the contrary to Louge *et al.* (1991) and He and Simonin (1993), we consider the algebraic closure model for the transport equations of polydispersed solid admixture in the pipe-jet flow in

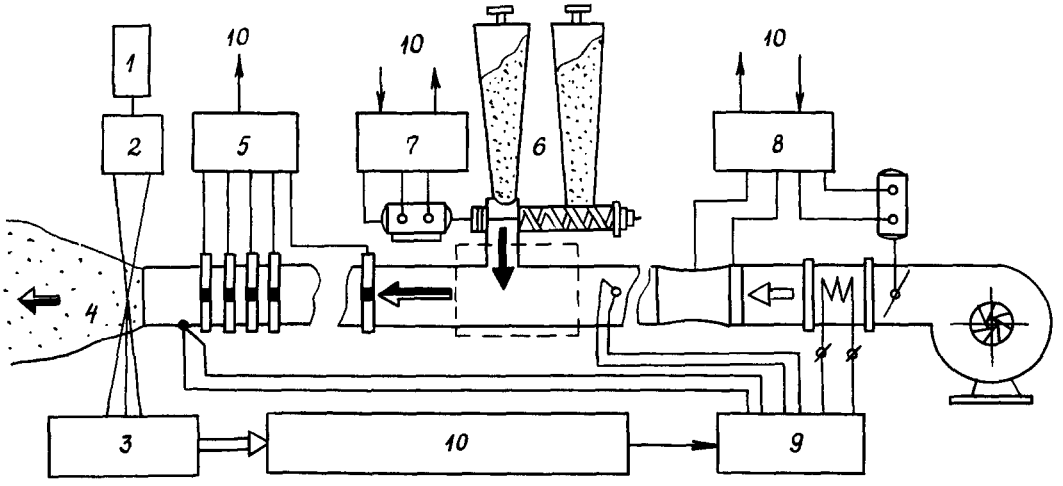

Figure 1. Aerodynamical bench: (1) laser He–Ne; (2) sending optics; (3) receiving optics; (4) test section; (5) pressure converter; (6) particle screw feeder; (7) dispersed phase dosimeter; (8) flowmeter; (9) thermocontroller; (10) registering processing and controlling system; (11) blower.

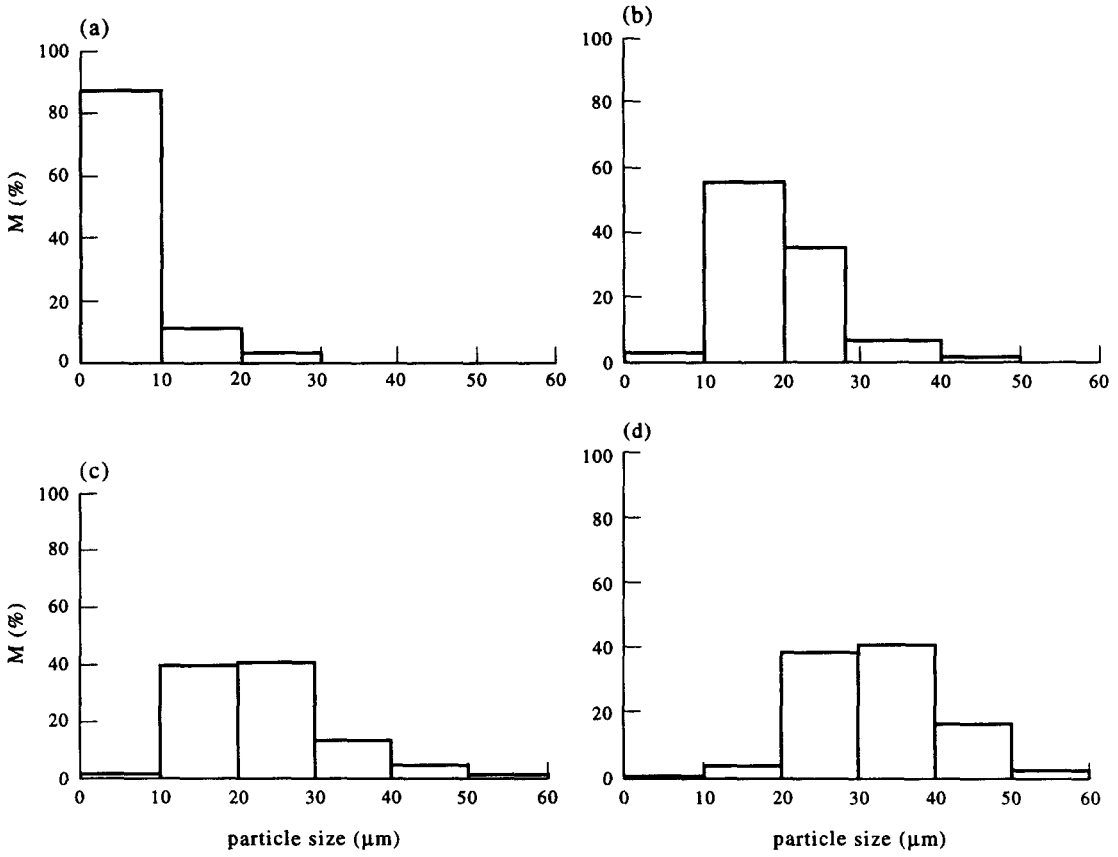

Figure 2. The particle mass distributions for various average particles diameters: (a) $\delta = 7\ \mu m$; (b) $\delta = 17\ \mu m$; (c) $\delta = 23\ \mu m$; (d) $\delta = 32\ \mu m$.

our article. Due to the force factors (in our model we consider the drag viscous force, the Magnus and Saffman lift forces) and also the turbophoresis force, the obtained radial velocity of the dispersed phase differs noticeably from the radial velocity of the gaseous phase. In that case there is no need to apply the hypothesis of the velocity equilibrium in the radial direction as it has been made by Abramovich *et al.* (1972), Vasilkov (1976) and Melville and Bray (1979) in the calculations of the transfer processes in free round two-phase turbulent jets. The initial conditions for the jet are defined by the calculated velocity and concentration fields of both phases in the pipe flow (at the outlet of the pipe). By this approach we can describe satisfactorily the pinch-effect of solid admixture experimentally found by Laats and Frishman (1970), and Navoznov *et al.* (1979).

2. EXPERIMENTAL FACILITY AND TECHNIQUES

The pinch and scattering effects of the dispersed phase discovered by Laats and Frishman (1970) and Navoznov *et al.* (1979) in a two-phase round turbulent jet were related to the anomalous phenomena and could not be explained. Therefore, they were checked repeatedly with applying various experimental facilities both in the horizontal and vertical jets using different experimental techniques. One of the experimental facilities designed for measurements in a pipe and jet is shown in figure 1. In the work by Laats and Frishman (1970) the particle mass flow rate was measured by an isokinetic sampling tube with a diameter of 2 mm. The injected air passed through the rotameter and solid admixture precipitated on the filter and was then weighed after a definite period of time. The gas velocity in various locations of the jet was calculated from the rotameter readings and the flow rate of the dispersed phase through the element (specific flow rate $kg/s \cdot m^2$) was measured by weighing the samples. In the work of Navoznov *et al.* (1979) the relative particle mass concentration was determined by the LDA technique. Moreover, in the work of Frishman *et al.*

(1993) the concentration was determined by direct counting of particles, which passed through the LDA measuring volume. Nevertheless, the pinch-effect observed for the motion of fine solid particles and scattering effect related with the motion of large solid particles were registered in all series of experiments. The experimental rig where the investigations in a pipe and jet flow were carried out is shown in figure 1. The aerodynamical rig consisted of the following main parts: a pipe for the formation and transportation of a two-phase flow and a test section. Besides, the aerodynamical rig included a blower, a particle screw feeder and also optical, registering, controlling and processing systems. The length of the pipe used in our experiments was about 6 m for various pipe diameters (15–35 mm). We conducted our experiments for various mean gas velocities of 30–50 m/s. The mass loadings were 0.3–0.62 kg dust/kg air. We investigated two-phase flows with 7, 17, 23 and 32 μm manufactured abrasive electrocorundum powders (Al_2O_3; $\rho_p = 3950$ kg/m^3). Since the physical properties of the dispersed systems depend significantly on the fractional composition of powders, it is necessary to know the distributions of particle sizes. The analysis of the polydispersity of applied powders shows that the root-mean-square deviation from the average particle size for the electrocorundum powder is no more than 30% of middle size of the particles.

The distributions of local averaged parameters (velocity and particle mass concentration) of the two-phase flow in various cross-sections of the pipe and jet were measured with the help of a forward-scatter laser Doppler anemometer (LDA) and laser concentration measurer (LCM) (He–Ne laser, sending and receiving optics in figure 1). The measurements of the particle mass concentration were based on measuring the light intensity of the beam scattered at some angle and the attenuated direct beam in the optical heterogeneous medium. The optical parts of LDA and LCM were installed on a special traversing device controlled by a PC-286. This allowed to scan the flow continuously or discretely in any given direction with the accuracy of 0.1 mm. The optical system included a 35 mW He–Ne laser. The LDA receiving optics contained two channels: one channel was tuned for registering signals from small flow tracers and the second for measuring the dispersed phase. Each channel consisted of receiving optics, fiber cable, photomultiplier (PM) and a special counter processor. Tuning of channels was based on the amplitude discrimination of the Doppler signals. The channel of the dispersed phase was tuned for registering signals only from the particles of this phase by selecting the geometry of the reception system and sensitivity of PM.

3. THE MODEL

The numerical calculation of the two-phase turbulent pipe-jet flow is based on the Euler approach employed for the dispersed phase, which is considered as a multi-velocity continuous phase (Nigmatilin's method of space averaging (1990) is applied), since the dispersed phase is considered here a polyfractional dispersed phase. The real manufactured powders of solid particles used in the experiments of Laats and Frishman (1970) and Navoznov *et al.* (1979) are made of

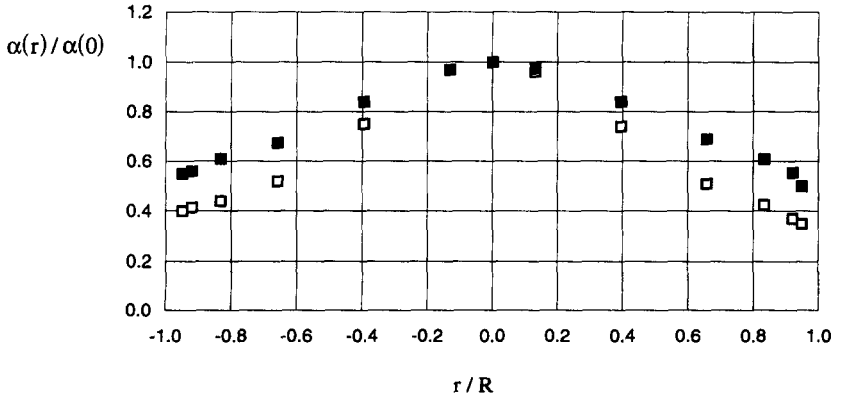

Figure 3. Distribution of particle mass concentration along the diameter at the pipe outlet for the following flow conditions: the mean velocity of gas $u = 50$ m/s, the pipe diameter $D = 15.2$ mm, the mass loading of 0.62 kg dust/kg air for two particle sizes: □ ($\delta = 23$ μm), ■ ($\delta = 32$ μm).

polyfractional dispersed material. Figure 2 shows the particle mass distributions for various mean particle diameters ($\delta = 7$, 17, 23 and 32 μm).

In the mathematical description the distribution of the particle mass concentration against the particle size is modelled by the finite number of the fractions characterized by their size, concentration. Polydispersity of the solid phase leads to collisions between particles from different fractions in their motion. In order to take into account the impact of collisional effect at the motion of the polyfractional solid admixture, we introduce the pseudo-viscosity coefficients. For simplifying the calculations, the polydispersed phase is modelled by three particle fractions: the main fraction (index 2) with a mass contribution of 50% from the total mass of particles of all fractions and two additional particle fractions with equal mass fractions (25%). This mass is less than that of the main fraction and with the particle size smaller (index 1) and larger (index 3) than the particle size of the main fraction. The difference between the particle sizes of fraction 1 and fraction 2 is 15%. Between fraction 3 and fraction 2 the difference is 8% of the particle size in the main fraction being identical for all considered particles. Therefore, the dispersed phase is characterized by the following parameters: the particle sizes of the fractions $\delta_1 < \delta_2 < \delta_3$; the velocity components u_{s1}, v_{s1}, u_{s2}, v_{s2}, u_{s3}, v_{s3} in the axial and radial directions, respectively; the angular velocity components ω_{s1}, ω_{s2}, ω_{s3} and mass concentrations α_1, α_2, α_3. The indices s1, s2, s3 show the parameters for different particle fractions, in particular, ω_{s1}, ω_{s2}, ω_{s3} are the angular velocities of fractions 1, 2, 3, respectively. We consider the two-dimensional, axysimmetrical pipe-jet flow and vector of the angular velocity has one component, which is oriented to the circumferential plane. We write the transport equations for the gaseous and dispersed phases in the approximation of the two-phase turbulent boundary layer neglecting the diffusive terms in the main flow direction (in our case in the axial direction) and keeping them in the transversal direction. The system of the transport equations of mass, momentum (in the axial and radial directions) and angular momentum is written for each particle fraction with taking into account the introduced pseudo-viscosity coefficients characterizing the additional (collisional) transfer of these substances. For the closure of transport equations of the dispersed phase the eddy-viscosity concept is used. The formulae for the pseudo-viscosity coefficients contain the linear and angular velocities and mass concentrations of each particle fraction. The formulae for the coefficients are obtained from the consideration of binary collision between particles (Chapman and Cowling 1970) and with taking into account the probability of the collisions of particles from different fractions (Trushin and Lipatov 1963).

Moreover, we have considered the influence of the turbulent fluctuations of the carrier gas flow on the motion of the dispersed phase. The additional terms—in the diffusion coefficient presented as a superposition of the diffusion pseudo-viscosity coefficient (originated from the particle collision) and the coefficient of the turbulent diffusion of particles in the transport equations of the translational momentum in the axial and radial directions and in the transport of the angular momentum—describe the influence of the gaseous phase on the motion and distribution of the dispersed phase in a pipe and jet. One of the additional terms in the equation of the momentum transfer in the radial direction describing the diffusion of the normal component of stress tensor of the dispersed phase includes the turbophoresis force, which results from the non-uniform distribution of the fluctuation energy of particles. Fletcher (1967) and Fortier (1967) were the first to pay attention to this effect. For the motion of a single particle, the given force was written by Gorbis and Spokoinyi (1977) and Mednikov (1981). According to the latter, this force is

$$-0.5 m_p \frac{1}{r} \frac{\partial}{\partial r} r \langle v_p'^2 \rangle.$$

The expression for the turbophoresis force written for a single particle with the motion of the dispersed phase as whole is transformed using the method of space averaging by Nigmatulin (1990):

$$-0.5 \rho_s \frac{1}{r} \frac{\partial}{\partial r} r \langle v_p'^2 \rangle.$$

The additional terms in the transport equations of the momentum in the axial direction characterize

the influence of that force caused by the turbulent transfer of the shear stress of the dispersed phase

$$-\rho_s \frac{1}{r}\frac{\partial}{\partial r} r\langle u_p' v_p' \rangle$$

and in the transport equation of the angular momentum—the turbulent transfer of the angular fluctuating velocity

$$-\rho_s \frac{1}{r}\frac{\partial}{\partial r} r\langle \omega_p' v_p' \rangle.$$

They describe the momentum exchange of particles with the carrier flow for the fluctuating motion. The formulae for the Euler correlations of the dispersed phase $\langle u_p' v_p' \rangle$, $\langle v_p'^2 \rangle$, $\langle \omega_p' v_p' \rangle$ and for the turbulent diffusion coefficient of particles were obtained by Shraiber *et al.* (1990). The average transport equations were written on the basis of the Euler approach, which Shaiber *et al.* (1990) used for obtaining the correlations of $\langle u_p' v_p' \rangle$, $\langle v_p'^2 \rangle$, $\langle \omega_p' v_p' \rangle$. They are the following:

$$\frac{\partial u_p}{\partial t} + u_p \frac{\partial u_p}{\partial x} + v_p \frac{\partial u_p}{\partial y} + \left\langle u_p' \frac{\partial u_p'}{\partial x} \right\rangle + \left\langle v_p' \frac{\partial u_p'}{\partial y} \right\rangle = \gamma(u - u_p) + \frac{\gamma_0}{[(u-u_p)^2 + (v-v_p)^2]}$$

$$\times [(u-u_p)\langle (u'-u_p')^2 \rangle + (v-v_p)\langle (u'-u_p')(v-v_p') \rangle] + \lambda_\omega (v - v_p)\left[\omega_p - \frac{1}{2}\left(\frac{\partial v}{\partial x} - \frac{\partial u}{\partial y} \right) \right]$$

$$+ \lambda_\omega \left\langle (v' - v_p') \left(\omega_p' - \frac{1}{2}\left(\frac{\partial v'}{\partial x} - \frac{\partial u'}{\partial y} \right) \right) \right\rangle, \qquad [1]$$

$$\frac{\partial v_p}{\partial t} + u_p \frac{\partial v_p}{\partial x} + v_p \frac{\partial v_p}{\partial y} + \left\langle u_p' \frac{\partial v_p'}{\partial x} \right\rangle + \left\langle v_p' \frac{\partial v_p'}{\partial y} \right\rangle = \gamma(v - v_p) + \frac{\gamma_0}{[(u-u_p)^2 + (v-v_p)^2]}$$

$$\times [(v-v_p)\langle (u'-u_p')(v-v_p') \rangle + (v-v_p)\langle (v'-v_p')^2 \rangle] - \lambda_\omega (u - u_p)\left[\omega_p - \frac{1}{2}\left(\frac{\partial v}{\partial x} - \frac{\partial u}{\partial y} \right) \right]$$

$$- \lambda_\omega \left\langle (u' - u_p') \left(\omega_p' - \frac{1}{2}\left(\frac{\partial v'}{\partial x} - \frac{\partial u'}{\partial y} \right) \right) \right\rangle, \qquad [2]$$

$$\frac{\partial \omega_p}{\partial t} + u_p \frac{\partial \omega_p}{\partial x} + v_p \frac{\partial \omega_p}{\partial y} + \left\langle u_p' \frac{\partial \omega_p'}{\partial x} \right\rangle + \left\langle v_p' \frac{\partial \omega_p'}{\partial y} \right\rangle = \beta_\omega \left[\frac{1}{2}\left(\frac{\partial v}{\partial x} - \frac{\partial u}{\partial y} \right) - \omega_p \right], \qquad [3]$$

where the coefficients are

$$\gamma = \frac{18\rho}{\rho_p}\frac{\nu}{\delta^2}(1 + b_1\sqrt{\mathrm{Re}_p} + b_2 \mathrm{Re}_p), \quad \gamma_0 = \frac{18\rho}{\rho_p}\frac{\nu}{\delta^2}\left(\frac{b_1}{2}\sqrt{\mathrm{Re}_p} + b_2 \mathrm{Re}_p \right),$$

$$\lambda_\omega = \frac{3\rho}{4\rho_p}, \quad \beta = \frac{18\rho\nu}{\rho_p \delta^2}, \quad \beta_\omega = \frac{60\rho}{\rho_p}\frac{\nu}{\delta^2}$$

and Re_p is the particle's Reynolds number. The inverse value of β is the dynamic relaxation time of the Stokes particle. Here the numerical constants $b_1 = 0.276$ and $b_2 = 0.139$ have been taken from Kravtsov's investigations (1968). The variables u, v, u_p, v_p, ω_p are the average translation and angular velocities of the gaseous and dispersed phases. On the ground of these equations and taking into account the expression for the Euler correlation of velocities of the carrier fluid and calculating the trajectory of particles in their fluctuating motion, Shraiber *et al.* (1990) obtained the formulae for sought correlations and for the coefficient of the turbulent diffusion of particles,

which are the following:

$$\langle v_p'^2\rangle = \frac{\gamma_{yy}^{0^2}\langle v'^2\rangle}{\gamma_{yy}(\gamma_{yy}+\varphi_{yy})} + \frac{\gamma_{yx}^{0^2}\langle u'^2\rangle}{\gamma_{yy}(\gamma_{yy}+\varphi_{xx})} + \frac{2\gamma_{yy}^0\gamma_{yx}^0\langle u'v'\rangle}{\gamma_{yy}(y_{yy}+\varphi_{xy})}, \quad [4]$$

$$\langle u_p'v_p'\rangle = \frac{(\gamma_{xx}^0\gamma_{yx}^0+\gamma_{yx}^0\gamma_{yx}^0)(\gamma_{xx}+\gamma_{yy}+2\varphi_{xy})}{(\gamma_{xx}+\gamma_{yy})(\gamma_{xx}+\varphi_{xy})(\gamma_{yy}+\varphi_{xy})}\langle u'v'\rangle + \frac{1}{(\gamma_{xx}+\gamma_{yy})}$$

$$\times\left[\frac{\gamma_{xy}^0\gamma_{yy}^0(\gamma_{xx}+\gamma_{yy}+2\varphi_{yy})\langle v'^2\rangle}{(\gamma_{xx}+\varphi_{yy})(\gamma_{yy}+\varphi_{yy})} + \frac{\gamma_{xx}^0\gamma_{yx}^0(\gamma_{xx}+\gamma_{yy}+2\varphi_{xx})\langle u'^2\rangle}{(\gamma_{xx}+\varphi_{xx})(\gamma_{yy}+\varphi_{xx})}\right], \quad [5]$$

$$\langle\omega_p'v_p'\rangle = -\frac{\beta_\omega\gamma_{yy}^0(\beta_\omega+\gamma_{yy}+2C_{t1}\varphi_{xy})}{2(\beta_\omega+\gamma_{yy})(\beta_\omega+C_{t1}\varphi_{xy})(\gamma_{yy}+C_{t1}\varphi_{xy})}\left\langle\frac{\partial u'}{\partial r}v'\right\rangle$$

$$-\frac{\beta_\omega\gamma_{yx}^0(\beta_\omega+\gamma_{yx}+2C_{t1}\varphi_{xx})}{2(\beta_\omega+\gamma_{yy})(\beta_\omega+C_{t1}\varphi_{xx})(\gamma_{yy}+C_{t1}\varphi_{xx})}\left\langle\frac{\partial u'}{\partial r}u'\right\rangle, \quad [6]$$

$$D_p = \frac{2C_{t2}k^{2.5}}{3\epsilon\left(\sqrt{\frac{2}{3}k}+V_r\right)^2}\left\{\left(\sqrt{\frac{2}{3}k}+\frac{V_r}{2}\right)\left[1+\left(\frac{\gamma_{yx}^0}{\gamma_{yy}^0}\right)^2\right]+\frac{1}{2V_r}\left[v_r^2+u_r^2\left(\frac{\gamma_{yx}^0}{\gamma_{yy}^2}\right)^2\right]\right\}$$

$$+\frac{2\gamma_{yx}^0}{\varphi_{xy}^0\gamma_{yy}^0}\langle u'v'\rangle, \quad [7]$$

where γ_{ij}, γ_{ij}^0 are the coefficients in the Eulerian and Lagrangian equations of the fluctuating motion of a particle related inversely proportionally to the time of the dynamic relaxation of Stokes particles, respectively; φ_{ij} is the exponent of the Euler correlation of the gas parameters at the fixed point, its inverse value is the Eulerian integral time scale and φ_{ij}^0 is the exponent of the correlation of the gas parameters along the particle path, its inverse value is connected with the Lagrangian integral time scale. The coefficients γ_{ij} and γ_{ij}^0 are determined as

$$\gamma_{xx} = \gamma_{xx}^0 + \frac{\partial u_s}{\partial x}, \quad \gamma_{yy} = \gamma_{yy}^0 + \frac{\partial v_s}{\partial r}, \quad \gamma_{xx}^0 = \gamma + \frac{\gamma_0 u_r^2}{V_r^2}, \quad \gamma_{yy}^0 = \gamma + \frac{\gamma_0 v_r^2}{V_r^2},$$

$$\gamma_{xy}^0 = \gamma_0\frac{u_r v_r}{V_r^2} - \chi_\omega\left[\frac{1}{2}\left(\frac{\partial v}{\partial x}-\frac{\partial u}{\partial r}\right)-\omega_p\right], \quad \gamma_{yx}^0 = \gamma_0\frac{u_r v_r}{V_r^2} + \chi_\omega\left[\frac{1}{2}\left(\frac{\partial v}{\partial x}-\frac{\partial u}{\partial r}\right)-\omega_p\right].$$

The exponents φ_{xx}, φ_{yy} are determined as $\varphi_{xx} = u/\Lambda_E$, $\varphi_{yy} = 2\varphi_{xx}$, and it is considered that $\varphi_{xy} \approx \varphi_{yy}$ in the model of Shraiber *et al.* (1990). For the jet calculation, the space scale of turbulence is determined as $\Lambda_E = C_{t2}k^{2.5}/\epsilon$, where the numerical constant C_{t2} equals to 0.13. In this model it is suggested that $\varphi_{xy}^0 \approx \varphi_{yy}^0$, where

$$\varphi_{yy}^0 = \frac{\left(\varphi+\frac{V_r}{\Lambda_E}\right)^2}{\varphi+0.5\frac{V_r}{\Lambda_E}+\frac{v_r^2}{2\Lambda_E V_r}}$$

and the value φ is calculated as

$$\varphi = \frac{1}{\Lambda_E}\sqrt{\frac{2k}{3}}$$

while the total velocity difference is $V_r = \sqrt{(u-u_p)^2+(v-v_p)^2}$.

According to the model by Shraiber *et al.* (1990), the influence of the dispersed phase on the turbulence of the carrier flow has been taken into account in the additional terms of transport

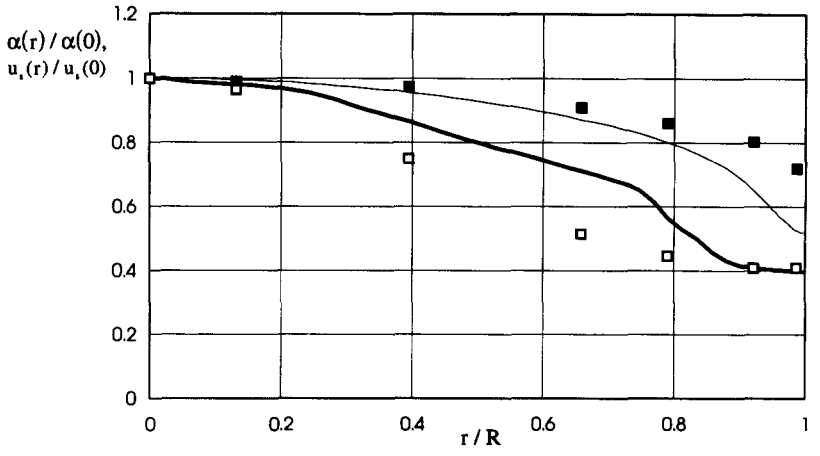

Figure 4. Distribution of particle mass concentration and particle velocity in the cross-section of the pipe outlet ($x/D = 200$) for the following flow conditions: the mean velocity of gas $u = 50$ m/s, the pipe diameter $D = 15.2$ mm, the particle size $\delta = 23$ μm, the mass loading of 0.62 kg dust/kg air: —, α (calc.); □, α (exp.); —, $u_s(r)/u_s(0)$ (calc.); ■, $u_s(r)/u_s(0)$ (exp.).

equations for the turbulent energy and the rate of its dissipation (the authors considered the two-way coupling), which are the following:

$$\epsilon_p \approx \frac{2\rho_s \gamma k}{3} \sum_3 \frac{\varphi_{ij}}{(\varphi_{ij} + \gamma_{ij})}, \qquad [8]$$

$$\Phi_p \approx \frac{2\rho_s \beta \epsilon C_{t1} \varphi_{xx}}{(C_{t1}\varphi_{xx} + \beta)}. \qquad [9]$$

Moreover, the viscous drag force, the Magnus and Saffman lift forces are also considered in our calculations. The expression for the Saffman force is generalized for the case of particle motion in a wide range of the Reynolds number of particles (Mei 1992). The Magnus lift force is the force acting on the rotating particles which move with the velocity lag (Rubinow and Keller 1961). The particles obtain angular velocities from their interaction with the walls as well as from the gradient of the gas velocity. Therefore, the transport equation for the angular momentum of the dispersed phase is added to the system of transport equations. In the presented model the influence of the gravitational force is insignificant. We consider that the motion of particles is balanced by the turbulent diffusion of particles, inter-particle collision effect and the Saffman lift force. The effect of particle collision as shown in the work of Sommerfeld and Zivcovic (1992) is important, yielding to the re-suspension of particles in a horizontal pipe. In our case for the transport of fine particles (7–32 μm) in a horizontal pipe, the settling velocity is lower than the velocity in radial direction by the factor of 10–100 resulted from the effect of inter-particle collision, the turbulent diffusion of particles and from the Saffman lift force. In addition, as our experiments showed, the profiles of particle mass concentration in the cross-section at the pipe outlet are axisymmetrical (figure 3). Therefore, we consider the axisymmetrical two-phase motion in the horizontal direction. In our calculations the other forces (i.e. Basset force, the force of added mass) are also neglected due to the low ratio of gas density to the density of particle material, which is less than 0.001.

4. EQUATIONS AND BOUNDARY CONDITIONS FOR THE GASEOUS DISPERSED PHASES IN THE PIPE AND JET FLOW

The transport equations of the gaseous and dispersed phases written in the two-phase turbulent boundary layer approximation are as follows:

$$\frac{\partial u}{\partial x} + \frac{1}{r}\frac{\partial (rv)}{\partial r} = 0, \qquad [10]$$

$$u\frac{\partial u}{\partial x}+v\frac{\partial u}{\partial r}=-\frac{\mathrm{d}P}{\rho\,\mathrm{d}x}+\frac{1}{r}\frac{\partial}{\partial r}r(\nu_t+\nu)\frac{\partial u}{\partial r}-\frac{18\rho\nu}{\rho_p}\sum_{i=1,3}\frac{C'_{Di}\alpha_i(u-u_{si})}{\delta_i^2}, \tag{11}$$

$$u\frac{\partial k}{\partial x}+v\frac{\partial k}{\partial r}=\frac{1}{r}\frac{\partial}{\partial r}r(\nu_t+\nu)\frac{\partial k}{\partial r}+\nu_t\left(\frac{\partial u}{\partial r}\right)^2-\epsilon-\epsilon_p-2\nu\left(\frac{\partial\sqrt{k}}{\partial r}\right)^2, \tag{12}$$

$$u\frac{\partial \epsilon}{\partial x}+v\frac{\partial \epsilon}{\partial r}=\frac{1}{r}\frac{\partial}{\partial r}r(\nu_t+\nu)\frac{\partial \epsilon}{\partial r}+\frac{C_{\epsilon 1}\epsilon\nu_t}{k}\left(\frac{\partial u}{\partial r}\right)^2-C_{\epsilon 2}\frac{\epsilon^2}{k}-\Phi_p+2\nu\nu_t\left(\frac{\partial^2 u}{\partial r^2}\right)^2, \tag{13}$$

$$\frac{\partial(\alpha_i u_{si})}{\partial x}+\frac{1}{r}\frac{\partial(r\alpha_i u_{si})}{\partial r}=\frac{1}{r}\frac{\partial}{\partial r}r(D_{si}+D_{pi})\frac{\partial \alpha_i}{\partial r}, \tag{14}$$

$$u_{si}\frac{\partial u_{si}}{\partial x}+\left(v_{si}-\frac{(D_{si}+D_{pi}+\nu_{si}^1)}{\alpha_i}\frac{\partial \alpha_i}{\partial r}\right)\frac{\partial u_{si}}{\partial r}=\frac{1}{r}\frac{\partial}{\partial r}r\left(\nu_{si}^1\frac{\partial u_{si}}{\partial r}-\langle u'_{pi}v'_{pi}\rangle\right)$$

$$+\frac{3\rho}{4\rho_p}\left[\frac{24C'_{Di}(u-u_{si})\nu}{\delta_i^2}-(v-v_{si})\Omega_i\right], \tag{15}$$

$$u_{si}\frac{\partial v_{si}}{\partial x}+\left(v_{si}-\frac{(D_{si}+D_{pi}+\nu_{si}^2)}{\alpha_i}\frac{\partial \alpha_i}{\partial r}\right)\frac{\partial v_{si}}{\partial r}=\frac{1}{r}\frac{\partial}{\partial r}r\left(\nu_{si}^2\frac{\partial v_{si}}{\partial r}-\langle v'^2_{pi}\rangle-k_{si}\right)$$

$$+\frac{3\rho}{4\rho_p}\left[\frac{24C'_{Di}(v-v_{si})\nu}{\delta_i^2}+(u-u_{si})\left(\Omega_i-\frac{4.1\cdot f(\mathrm{Re}_{pi},\mathrm{Re}_{si})\sqrt{\nu}}{\delta_i}\sqrt{\frac{\partial u}{\partial r}}\right)\right], \tag{16}$$

$$u_{si}\frac{\partial \omega_{si}}{\partial x}+\left(v_{si}-\frac{(D_{si}+D_{pi}+\nu_{si}^3)}{\alpha_i}\frac{\partial \alpha_i}{\partial r}\right)\frac{\partial \omega_{si}}{\partial r}=\frac{1}{r}\frac{\partial}{\partial r}r\left(\nu_{si}^3\frac{\partial \omega_{si}}{\partial r}-\langle \omega'_{pi}v'_{pi}\rangle\right)$$

$$-\frac{60\rho\nu}{\rho_p\delta_i^2}\Omega_i, \tag{17}$$

$$\nu_t=c_{\mu t}\frac{k^2}{\epsilon}, \tag{18}$$

where the rotational slip velocity is

$$\Omega_i=\frac{1}{2}\left(\frac{\partial v}{\partial x}-\frac{\partial u}{\partial r}\right)-\omega_{si},$$

and the function

$$f(\mathrm{Re}_{pi},\mathrm{Re}_{si})=\left(1-0.23434\frac{\mathrm{Re}_{si}}{\mathrm{Re}_{pi}}\right)\exp\left(-\frac{\mathrm{Re}_{pi}}{10}\right)+0.23434\frac{\mathrm{Re}_{si}}{\mathrm{Re}_{pi}}\ (\text{at } \mathrm{Re}_{pi}\leqslant 40),$$

$$f(\mathrm{Re}_{pi},\mathrm{Re}_{si})=0.0371\sqrt{\mathrm{Re}_{si}}\ (\text{at } \mathrm{Re}_{pi}>40),$$

is determined according to Mei (1992) and

$$\mathrm{Re}_{si}=\left|\frac{\partial u}{\partial r}\right|\frac{\delta_i^2}{4\nu};$$

v, v_t are the kinematic and turbulent viscosity, respectively; ρ, ρ_p are the gas and the particle material densities, respectively.

In order to obtain the formulae for the pressure gradient and radial velocity of the gaseous phase, we solve the continuity equation of the gaseous phase [10] together with the transport equation of the momentum of this phase [11] using the method by Abramovich *et al.* (1984) and obtain the following expressions:

$$\frac{dP}{\rho\, dx} = \frac{\int_0^R \frac{1}{u^2}\left(\frac{\partial}{\partial r} r(v_t + v)\frac{\partial u}{\partial r}\right)dr - \frac{18\rho v}{\rho_p \delta_i^2}\int_0^R \frac{\alpha_i C'_{Di}(u - u_{si})r\, dr}{u^2}}{\int_0^R \frac{r\, dr}{u^2}}, \quad [19]$$

$$v = \frac{u}{r}\left\{-\int_0^r \frac{1}{u^2}\left(\frac{\partial}{\partial r} r(v_t + v)\frac{\partial u}{\partial r}\right)dr + \frac{dP}{\rho\, dx}\int_0^r \frac{r\, dr}{u^2} + \frac{18\rho v}{\rho_p \delta_i^2}\int_0^r \frac{\alpha_i C'_{Di}(u - u_{si})r\, dr}{u^2}\right\}. \quad [20]$$

We use the k–ϵ turbulence model, including the transport equations of the turbulent energy [12] and its rate of dissipation [13] and an expression for the coefficient of the turbulent viscosity [18]. We consider the two-way coupling expressed through the influence of additional forces in the [12] and [13]. The additional terms ϵ_p, Φ_p ([8] and [9]) are given on the right-hand side of these equations, respectively. The wall functions $C_{\epsilon 1}$, $C_{\epsilon 2}$, $c_{\mu t}$ are determined according to Durst and Rastogi (1972) as follows:

$$C_{\epsilon 1} = 1.55,\ C_{\epsilon 2} = 2\cdot(1 - 0.3\cdot\exp(-\mathrm{Re}_t^2)),$$

$$c_{\mu t} = 0.07\cdot\exp\left[-\frac{2.5}{\left(1 + \frac{\mathrm{Re}_t}{50}\right)}\right],$$

where the turbulent Reynolds number is $\mathrm{Re}_t = k^2/v\epsilon$.

Using the eddy-viscosity concept, the stress tensor components for the dispersed phase are expressed through the rate of the shearing strain and the introduced pseudo-viscosity coefficients given in the diffusive terms of the transport equations [14]–[17] like it was presented by He and Simonin (1993):

$$\langle u'_{si} v'_{si}\rangle = -v^1_{si}\frac{\partial u_{si}}{\partial r}, \quad [21]$$

$$\langle v'_{si} v'_{si}\rangle = -v^2_{si}\frac{\partial v_{si}}{\partial r} + \frac{2}{3}k_{si}, \quad [22]$$

$$\langle \omega'_{si} v'_{si}\rangle = -v^3_{si}\frac{\partial \omega_{si}}{\partial r}, \quad [23]$$

$$\langle \alpha'_i v'_{si}\rangle = -D_{si}\frac{\partial \alpha_i}{\partial r}. \quad [24]$$

Here the fluctuating variables result from the inter-particle collision in the polyfractional dispersed flow. The expression [22] is derived from the generalized form of the stress tensor for the normal component of the dispersed phase like in He and Simonin (1993). The parameter k_{si} describes the exchange of kinetic energy between the particles of the ith fraction with the particles from other particle fractions of the dispersed phase at their interaction.

On the right-hand side of transport equations, which are written for each particle fraction (index $i = 1, 3$) for the momentum of the dispersed phase in the axial [15] and radial directions [16] the influence of the viscous drag force (the second term), the Magnus and Saffman lift forces (the third

and fourth terms) are taken into account. On the right-hand side of the transport equation of the angular momentum of the dispersed phase [17], the second term describes the decay rate of the angular velocity of particles due to the viscosity of the surrounding gas (Rubinow and Keller 1961). On the right-hand side of the transport equations for the mass, momentum and angular momentum [14], [15], [16], [17], respectively, the influence of turbulence of the gaseous phase is taken into account, which is expressed through the terms for the turbulent diffusion coefficient of particles D_{pi}, and through the diffusion of the Eulerian correlation $\langle u'_{pi}v'_{pi}\rangle$, $\langle v'^2_{pi}\rangle$, $\langle \omega'_{pi}v'_{pi}\rangle$. All these equations are written for the dispersed phase with taking into account the procedure of space averaging by Nigmatulin (1990).

The fields of the gaseous phase are calculated along the length of the pipe ($L = 50D$) up to the injection of particles into the pipe. Thus, we have had a fully developed, steady gas flow before we started the calculation of the parameters of the dispersed phase (according to our experiments). For the calculations of gas fields, the initial conditions are taken similar to Durst and Rastogi (1977) with the uniform top hat profiles for the axial velocity component, for turbulent energy and for the dissipation rate of turbulent energy. The particles enter the pipe with the initial velocity given as 15% of the velocity of the gaseous phase with the uniform distribution in the cross-section. The uniform distribution of the particle mass concentration for each fraction is also given in the initial cross-section and the radial and angular velocities of the dispersed phase in the initial field are taken zero. Thus, the initial conditions for the parameters of the dispersed phase are as follows:

$$x = 0 \quad u_{si} = 0.15 \cdot u|_{r=0}, \quad \alpha_2 = 0.5 \cdot \chi, \quad \alpha_1 = \alpha_3 = 0.25 \cdot \chi, \; v_{si} = 10^{-5}, \; \omega_{si} = 10^{-5}. \qquad [25]$$

The boundary conditions for the gaseous phase are standard—non-slip conditions for axial and radial velocity components (for the impenetrable wall) and the same as for the turbulent energy and its rate of dissipation. We take symmetry conditions for these parameters at the axis. Thus, they are

at the axis

$$\frac{\partial u}{\partial r} = \frac{\partial k}{\partial r} = \frac{\partial \epsilon}{\partial r} = v\Big|_{r=0}, \qquad [26]$$

at the wall

$$u = v = k = \epsilon|_w = 0. \qquad [27]$$

The parameters for the dispersed phase are written with assuming the slip velocity conditions along the wall analogous to the theory of rarefied gases (Chapman and Cowling 1970). We consider no losses for the particle interaction with the wall (no rebound effect). For the description of the motion of large solid particles in a horizontal channel with the slip velocity between the gaseous and dispersed phases in the main flow direction, the mathematical model of the saltating motion of large particles was elaborated, which took into account the rebound effect, in addition to the other factors (Hussainov *et al.* 1996). The influence of the restitution and friction coefficients describing the particle-wall interaction is estimated in our work as well. As our calculations based on that so-called saltating model of particle motion showed, the rebound effect plays no significant role in the motion of fine particles in a horizontal pipe, and therefore we consider that the particles slide along the wall without interaction, without friction. We set nonzero velocity conditions at the wall—the gradient boundary conditions for the axial and angular velocities of particles. We set impenetrable velocity condition for the radial velocity of both phases at the wall. For the particle mass concentration, the boundary condition can be obtained from the transport equation for the particle mass if to integrate the particle mass flow rate over the cross-section of a pipe. So, we can write the boundary conditions for the velocities and mass concentration:

at the axis

$$\frac{\partial u_{si}}{\partial r} = \frac{\partial \alpha_i}{\partial r}\Big|_{r=0} = 0, \quad v_{si} = \omega_{si}|_{r=0} = 0, \qquad [28]$$

at the wall

$$\left.\frac{\partial u_{si}}{\partial r}\right|_w = \left.\frac{\partial \omega_{si}}{\partial r}\right|_w = 0; \quad v_{si}|_w = 0; \quad \alpha_{si} v_{si}|_w = D_{si} \left.\frac{\partial \alpha_{si}}{\partial r}\right|_w. \tag{29}$$

The transport equations and boundary conditions for the round turbulent two-phase jet can be written then in new coordinates. Since the jet expands, we must transform the widening area into the rectangular area as it was done by Krasheninnikov (1972). So, in the new coordinate system the transport equations of both phases can be written using the new variables determined as $x = \bar{x} \cdot R$, $\eta = \bar{\eta} \cdot R$, where $\bar{x}$, $\bar{\eta}$ are the dimensionless variables and

$$\bar{\eta} = \frac{\bar{r}}{(1 + T \cdot \bar{x})} = \frac{\bar{r}}{AA}, \quad \bar{r} = \frac{r}{R}$$

(R is the pipe radius). The initial conditions for both phases are obtained as a result of the calculation of the two-phase flow in the pipe. The boundary conditions for the gaseous phase in case of the round jet are, as follows:
at the axis

$$\frac{\partial u}{\partial \eta} = \frac{\partial k}{\partial \eta} = \frac{\partial \epsilon}{\partial \eta} = v\Big|_{\eta = 0} = 0, \tag{30}$$

at the outer border of the jet (∞):

$$u|_\infty = 0.045 u|_{r=0}, \quad k|_\infty = 10^{-4}(u|_{r=0})^2, \quad \epsilon|_\infty = 10^{-6}\frac{(u|_{r=0})^3}{R}, \quad \left.\frac{\partial v}{\partial \eta}\right|_{\eta = \infty} = 0. \tag{31}$$

The boundary conditions for the dispersed phase are:
at the axis

$$\frac{\partial u_{si}}{\partial \eta} = \left.\frac{\partial \alpha_i}{\partial \eta}\right|_{\eta = 0} = 0, \quad v_{si} = \omega_{si}|_{\eta = 0} = 0, \tag{32}$$

at the outer border (∞):

$$u_{si}|_\infty = 0.045 u|_{r=0}, \quad v_{si}|_\infty = -10^{-5} u|_{r=0}, \quad \left.\frac{\partial \omega_{si}}{\partial \eta}\right|_\infty = 0, \quad \alpha_i|_\infty = 0.045 \cdot \alpha_i|_w. \tag{33}$$

The jet boundaries are not set beforehand, but are chosen according to the requirement of smooth transformation of the parameters of two-phase flow at the outer boundary of the jet (∞) as by Brailovskaja and Chudov (1962). The smooth transformation can be obtained when the following condition is satisfied:

$$\left.\frac{\partial u}{\partial \eta}\right|_{\to \infty} \leqslant K u|_{r=0}, \tag{34}$$

where K is the numerical constant and $K = 0.05$.

The system of transport equations of the pipe-jet flow is the system of parabolic equations of two-phase turbulent boundary layer. This system can be solved by the numerical tri-diagonal matrix algorithm using the implicit scheme by writing the upwind derivations in the radial direction and a special form of the source term on the right-hand side of equations (Patankar 1980). We used unequal grid spacing in the approximation of derivatives in the radial direction near the wall.

5. PSEUDO-VISCOSITY COEFFICIENTS

For the definition of the pseudo-viscosity coefficients, let us assume the binary impact of two particles. The velocity differences for linear and angular components before and after collision with taking into account the recovery coefficients of such collision k_{np}, k_{tp} are presented in appendix A.

These velocity differences are considered as a part of the fluctuating velocities of particles originated from the inter-particle collisions. For obtaining the stress tensor components, let us multiply different components of fluctuating velocities and average this product over two angles φ, θ and the parameter χ defining the distance between the particle centers at their impact. The given approach with the geometrical interpretation of these variables has been considered by Babukha and Shraiber (1972) which the calculations have been made for the two-phase laminar boundary layer by Hussainov *et al.* (1995). As a result, we can get the following combinations: $\langle(u'_{sij} - u_{si})(v'_{sij} - v_{2si})\rangle|_{\theta,\chi,\varphi}$, $\langle(v'_{sij} - v_{si})^2\rangle|_{\theta,\chi,\varphi}$, $\langle(\omega'_{sij} - \omega_{si})(v'_{sij} - v_{si})\rangle|_{\theta,\chi,\varphi}$, $\langle[(u'_{sij} - u_{si})^2 + (v'_{sij} - v_{si})^2]\rangle|_{\theta,\chi,\varphi}$ and etc. The averaging procedure is as follows:

$$\langle(u'_{sij} - u_{si})(v'_{sij} - v_{si})\rangle|_{\theta,\chi,\varphi} = \frac{1}{2\pi}\frac{1}{\varphi_{ij}}\frac{\displaystyle\int_0^{2\pi} d\theta \int_0^1 \chi\, d\chi \int_0^{\varphi_{ij}} (u'_{sij} - u_{si})(v'_{sij} - v_{si}) d\varphi}{\displaystyle\int_0^1 \chi\, d\chi}. \quad [35]$$

Following this and dropping the cumbersome calculations (Hussainov *et al.* 1995), the formulae (in complete form) for different stress tensor components are presented in appendix B. These values depend strongly on the angle φ_{ij} of the averaging procedure, which is determined as

$$\varphi_{ij} = \left| \text{arctg} \left[\frac{\left(\frac{v_{si}}{u_{si}} - \frac{v_{sj}}{u_{sj}}\right)}{\left(1 + \frac{v_{si}}{u_{si}}\frac{v_{sj}}{u_{sj}}\right)} \right] \right|. \quad [36]$$

For the definition of pseudo-viscosity coefficients, let us multiply the obtained components of the stress tensor with the time of the inter-particle collision Δt. This time was determined by Marble (1964) and calculated in (Hussainov *et al.* 1995) through the probability of the particle collision. In the simplest case of the particle binary collision the probability of collision of a particle from the ith fraction with particles from other fractions can be obtained according to Trushin and Lipatov (1963) as follows:

$$P_{ij} = \frac{\pi}{4}\frac{(\delta_i + \delta_j)^2}{l_i^2}, \quad [37]$$

where l_i is the inter-particle distance for the ith particle fraction, which is determined by knowing the particle mass concentration α_i as

$$l_i = \delta_i \sqrt[3]{\frac{\pi\rho}{6\rho_p\alpha_i}}.$$

Estimating the probability of collision as at least one collision in the volume of 1 cm^3 during the time interval of 1 s, Trushin and Lipatov (1963) determined the probability of collision through geometrical parameters as a ratio of the cross-section of colliding particles to the square of inter-particle distance [37]. Sommerfeld and Zivkovic (1992) and later Sommerfeld (1995) determined the probability of collision, which obeys to the Poisson's distribution function. In both cases the probability of particle collision is small being about 0.01. Neglecting the cumbersome calculations and using the expressions

$$v_{si}^1 = \langle(u'_{sij} - u_{si})(v'_{sij} - v_{si})\rangle|_{\theta,\chi,\varphi}\Delta t, \quad v_{si}^2 = \langle(v'_{sij} - v_{si})^2\rangle|_{\theta,\chi,\varphi}\Delta t,$$

$$v_{si}^3 = \langle(\omega'_{sij} - \omega_{si})(v'_{sij} - v_{si})\rangle|_{\theta,\chi,\varphi}\Delta t, \quad D_{si} = [\langle(u'_{sij} - u_{si})^2\rangle + \langle(v'_{sij} - v_{si})^2\rangle]|_{\theta,\chi,\varphi}\Delta t),$$

we can write these pseudo-viscosity coefficients for three particle fractions ($i = 1, 3$, $j = 1, 3$) and

four transport equations $k = 1, 4$ as follows:

$$v_{si}^k = g_0 \sum_{j=1, j\neq i}^{3} \frac{\beta_{ji}^2}{\sqrt[3]{\alpha_j}} (V_i + V_j)\delta_j X_{ij}^k, \qquad [38]$$

where the coefficient

$$g_0 = \sqrt[3]{\frac{\pi\rho_p}{6\rho}}$$

and

$$\beta_{ji} = \frac{m_{pj}}{m_{pi} + m_{pj}}$$

is the ratio of the single particle mass to the total mass of colliding particles; $k = 1, 4$. Then the coefficients X_{ij}^k can be defined (in the complete form) in appendix C. Furthermore, we designate the pseudo-diffusion coefficient for various particle fractions as $D_{si} = v_{si}^4$.

The expression for the parameter k_{si}, which characterizes the exchange of kinetic energy at particle collision (the gain and loss of energy at the moment of the particle impact) can be obtained by multiplying the quadrate of the fluctuating velocity difference $\langle[(u'_{sij} - u_{si})^2 + (v'_{sij} - v_{si})^2]\rangle|_{\theta,\chi\varphi}$ (written in appendix A) to the probability of the particle collision [37], i.e. the probability of the collision of particles from the ith fraction with the particles from other particle fractions ($j = 1, 3$ and $j \neq i$). The expression written for each particle fraction k_{si} is as follows:

$$k_{si} = \sum_{j=1, j\neq i}^{3} \beta_{ji}^2 (V_i + V_j)^2 P_{ij} Y_{ij}, \qquad [39]$$

where the coefficients Y_{ij} are presented in appendix C. The restitution coefficient k_{np} is the coefficient relating the normal velocity component after collision to that before the collision and the friction coefficient k_{tp} is the coefficient relating the tangential velocity component after collision to that before the collision, are introduced in the formula for recalculation of the translation and angular velocities after particle collision described by Babukha and Shraiber (1972). In our calculation the restitution coefficient is taken (for all flow conditions) as $k_{np} = -1$ and the friction coefficient is taken as $k_{tp} = 0.31$.

Thus, according to the expressions of the obtained pseudo-viscosity coefficients, they take into account the properties of the flow expressed through linear and angular particle velocities and particle mass concentration, the relaxation parameters of particles (their size and material density) and the parameters of collision (the restitution and friction coefficients).

6. RESULTS AND DISCUSSION

The calculations of the two-phase turbulent pipe-jet flow were conducted to describe the peculiarities of the distributions of the particle mass concentration. They are expressed by various profiles of mass concentration in the cross-sections of a pipe and also by the pinch-effect of the distribution of solid admixture in the turbulent round jet observed for fine solid particles. The numerical results were compared with the experimental data obtained in our laboratory for various flow conditions: different sizes of electrocorundum ($\rho_p = 3950$ kg/m^3) particles ($\delta = 7$–32 μm), two pipe diameters ($D = 15.2$ and 35 mm), two mean velocities of the gaseous phase ($u = 30$ and 50 m/s) and two mass loadings (0.34 and 0.62 kg dust/kg air). According to our investigations, the criterial Stokes number satisfies the condition $\mathrm{Stk}_* < 3$. Such motion of fine solid particles is accompanied by the anomalous distribution of particle mass concentration (pinch-effect) in the jet. Here, the Stokes number is determined as

$$\mathrm{Stk}_* = \frac{2\rho_p}{9\rho}\delta^2 \mathrm{Re}_*,$$

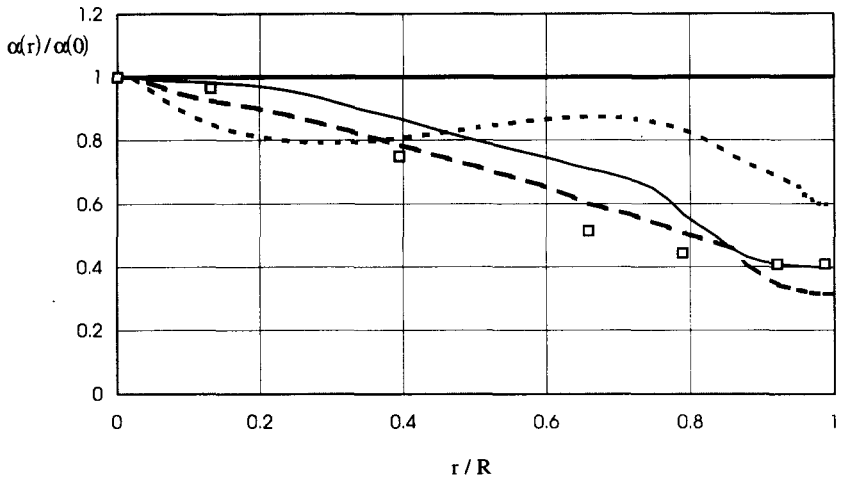

Figure 5. Distribution of particle mass concentration in various cross-sections of the pipe (flow conditions are the same as in figure 4.): —, $x/D = 0$; - - -, $x/D = 25$; – – –, $x/D = 100$; —, $x/D = 200$; □, α (exp.).

the relative particle diameter is $\delta = \delta/D$ and the Reynolds number determined via the friction velocity v_* is calculated as $\mathrm{Re}_* = v_* D/2\nu$. Hussainov *et al.* (1996) found that for the Stokes numbers larger than 3, the motion of solid particles in a pipe is characterized by the substantial velocity lag. For such motion in a pipe, the scattering effect expressed by the intensive dispersion of solid particles in the initial stage of the two-phase jet, has been found by Laats and Frishman (1970) and by Navoznov *et al.* (1979).

The profiles of relative particle mass concentration (related to its value at the pipe axis) and the velocities of the dispersed phase (in the dimensionless form) in the cross-section located downstream (at the length of 200 pipe diameters) are shown in figure 4 for the motion of 23 μm particles. The numerical results were compared with the experimental data obtained by Navoznov *et al.* (1979). It is shown that the profile of the particle mass concentration is non-uniform in the cross-section and has the maximum at the pipe axis. The transformation of the distribution of relative particle mass concentration in various cross-sections of the pipe (0, 25, 100 and 200 pipe diameters) is presented in figure 5 while the numerical results are compared with the experimental data for the pipe outlet. It can be seen that the uniform distribution of mass concentration obtained in the calculations for the initial cross-section (bold solid line) changes and becomes non-uniform across the pipe in fully developed, steady flow (thin solid curve in figure 5). At the non-steady flow region (25 pipe diameters downstream), the wavy distribution of particle mass concentration can be observed (the dashed curve). The distribution of particle velocities obtained from the numerical

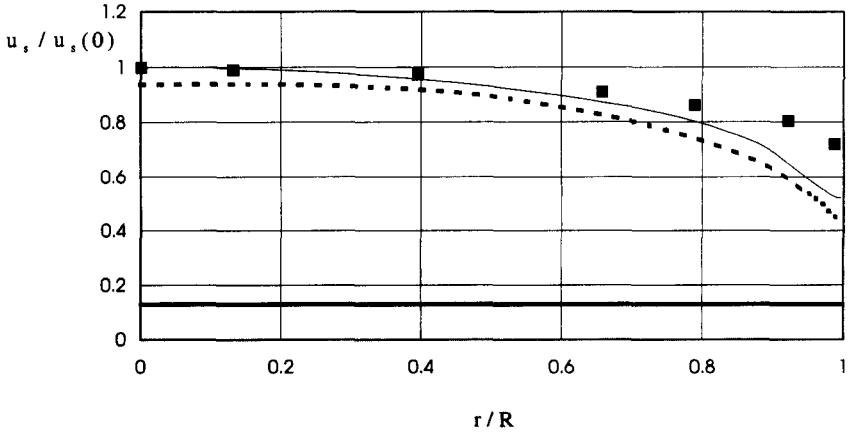

Figure 6. Distribution of particle velocity in various cross-sections of the pipe (flow conditions are the same as in figure 4.): —, $x/D = 0$; - - -, $x/D = 25$; —, $x/D = 200$; ■, $u_s(r)/u_s(0)$ (exp.).

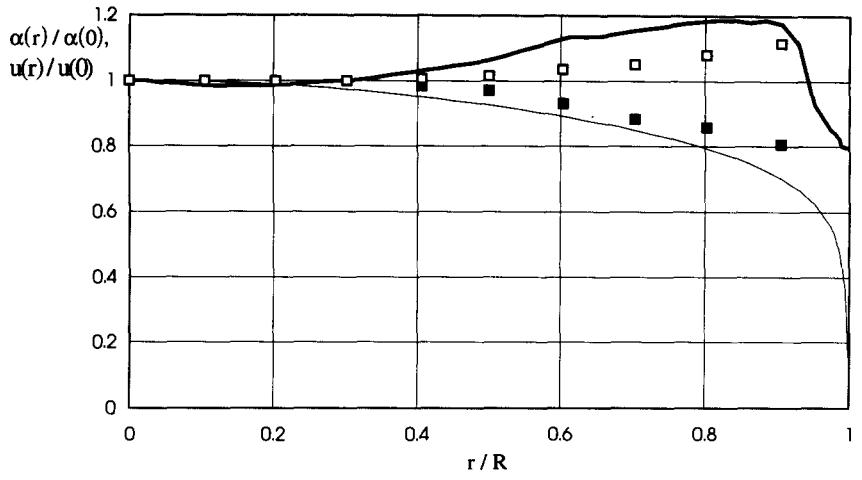

Figure 7. Distribution of particle mass concentration and the gas velocity in the cross-section of the pipe outlet ($x/D = 200$) for the following flow conditions: the mean velocity of gas $u = 50$ m/s, the pipe diameter $D = 35$ mm, the particle size $\delta = 17$ μm, the mass loading of 0.34 kg dust/kg air: —, α (calc.); □, α (exp.); —, $u(r)/u(0)$ (calc.); ■, $u(r)/u(0)$ (exp.).

calculations in various cross-sections of the pipe are presented in the dimensionless form in figure 6 and compared with the experimental data. In the calculations the initial distribution of particle velocity was taken uniform making 15% of the gas velocity at the axis. Fine particles are accelerated in the non-steady region of the pipe flow up to reaching the velocity of the gaseous phase where the particles move almost without any velocity lag in fully developed, steady flow. Thus, together with the changes in the distribution of the particle velocity along the pipe, the profiles of particle mass concentration are also transformed from the uniform distribution in the initial cross-section of the pipe to the non-uniform distribution in fully developed, steady region (thin curve in figure 5). The distribution of relative particle mass concentration and the velocity of the gaseous phase at the distance of 200 pipe diameters from the initial cross-section of the pipe are shown in figures 7 and 8 for other flow conditions: the motion of 17 and 32 μm particles in a pipe with the larger diameter of 35 mm, the mass loading of 0.34 kg dust/kg air and for the mean velocity of gas 50 m/s. The numerical results have been compared with the experimental data by Laats and Frishman (1970). The distributions of relative mass concentration at the cross-section of the pipe outlet for three sizes of particles: 7, 17 and 32 μm in a pipe with the diameter of 35 mm are shown in figure 9. As the experiments show, the motion of such fine particles has no velocity slip between the

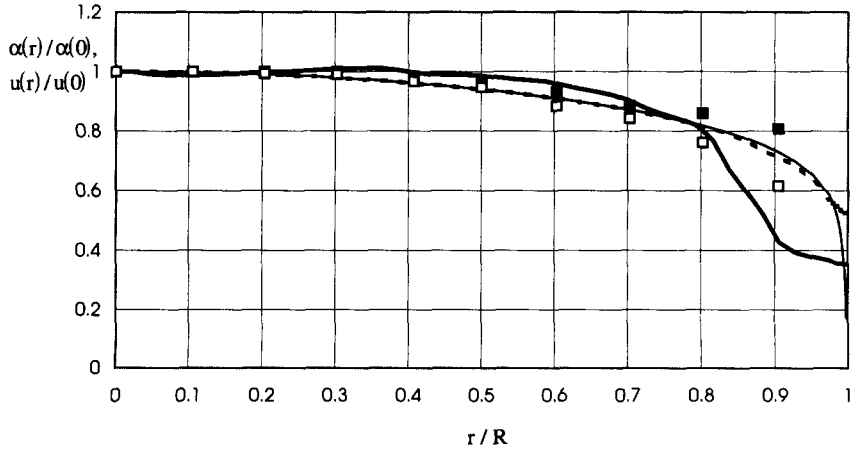

Figure 8. Distribution of particle mass concentration and the gas and particle velocity in the cross-section of the pipe outlet ($x/D = 200$) (flow conditions are the same as in figure 7) for the particle size $\delta = 32$ μm: —, α (calc.); □, α (exp.); —, $u(r)/u(0)$ (calc.); ■, $u(r)/u(0)$ (exp.); - - -, $u_s(r)/u_s$ (0) (calc.).

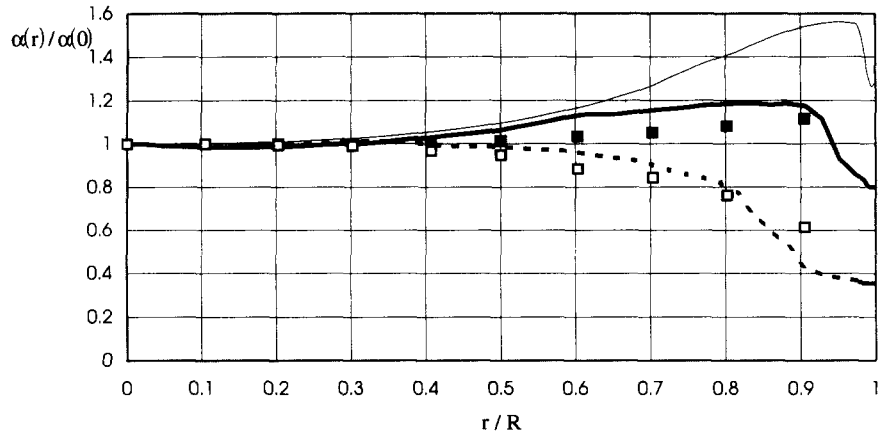

Figure 9. Distribution of particle mass concentration for various particle sizes in the cross-section of the pipe outlet ($x/D = 200$) (flow conditions are the same as in figure 7): —, $\delta = 7$ μm; —, $\delta = 17$ μm (calc.), ■, (exp.); - - -, $\delta = 32$ μm (calc.), □, (exp.).

gaseous and dispersed phases. The analysis of the distributions of the relative particle mass concentration in the pipe shows two regimes for the two-phase turbulent motion in these flows: the two-phase flow with very fine particles when $\mathrm{Stk}_* < 1$ ($\delta = 7, 17$ μm), and the two-phase flow with fine particles of larger sizes for $1 < \mathrm{Stk}_* < 3$ ($\delta = 23, 32$ μm). The upper limit for the Stokes number corresponds to the motion of large particles with the velocity slip in fully developed, steady flow in a horizontal channel (Hussainov *et al.* 1996). Two different regimes of the two-phase flow carrying fine solid particles are characterized by noticeably different distribution of mass concentration of solid admixture in the cross-section of a pipe. For the motion of very fine solid particles ($\delta = 7, 17$ μm) when $\mathrm{Stk}_* < 1$ the profile of the relative mass concentration is non-uniform with the maximum value near the wall. On the contrary, for the motion of fine solid particles with larger sizes (23, 32 μm) when $1 < \mathrm{Stk}_* < 3$, the profile of the relative mass concentration is non-uniform with the maximum value at the axis of the pipe. The analysis of force factors acting on the motion of solid particles in a pipe shows a significant role of the Saffman lift force, which depends on the velocity gradient $\partial u/\partial r$ and velocity lag $u - u_s$. This force dominates substantially near the wall resulting in the non-uniform distribution of concentration.

Now let us consider the velocity distribution of both phases, and the relative particle mass concentration in a two-phase turbulent round jet flowing out from the same pipe with the initial

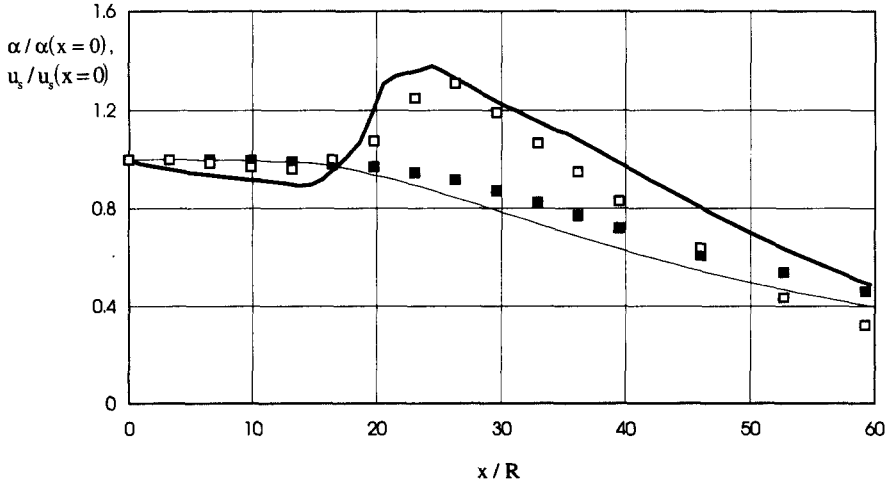

Figure 10. Distribution of particle mass concentration and the particle velocity along the axis of the two-phase jet for the following flow conditions: the mean velocity of gas at the pipe outlet $u = 50$ m/s, the pipe diameter $D = 15.2$ mm, the particle size $\delta = 23$ μm, the mass loading of 0.62 kg dust/kg air: —, $\alpha(x)/\alpha(x = 0)$ (calc.); □, $\alpha(x)/\alpha(x = 0)$ (exp.); —, $u_s(x)/u(x = 0)$ (calc.); ■, $u(x)/u_s(x = 0)$ (exp.).

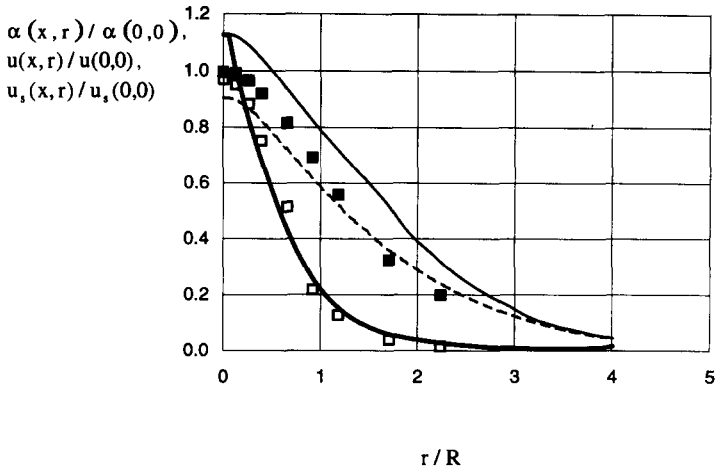

Figure 11. Distribution of particle mass concentration in the cross-section of the two-phase jet $x/D = 10$ (flow conditions are the same as in figure 10): —, $\alpha(r)/\alpha(0)$ (calc.); - - -, $u(r)/u(0)$ (calc); —, $u_s(r)/u_s(0)$ (calc.); □, $\alpha(r)/\alpha(0)$ (exp.); ■, $u_s(r)/u_s(0)$ (exp.).

distributions of these parameters obtained in the cross-section of the pipe outlet (200 pipe diameters from the inlet). The distribution of relative particle mass concentration and particle velocities in a two-phase jet along its axis and in three different cross-sections for the particles of 23 μm flowing out from the pipe with the diameter of 15.2 mm for two flow conditions, i.e. for two mean velocities of the outflow gas (30 and 50 m/s) are shown in figures 10–15. The numerical results have been compared with the experimental data obtained by Navoznov *et al.* (1979). The distribution of relative particle mass concentration and velocity of the dispersed phase along the axis for the particles of 23 μm with the mean outflow velocity of 50 m/s are shown in figure 10. At the distances of 10–15 pipe diameters from the pipe outlet the pinch-effect has been observed. Figure 10 shows that after the accumulation of admixture on the axis of the jet, which takes place approximately at 12 pipe diameters downstream, fading of the concentration begins, which proceeds downstream the jet. The distribution of the same flow parameters is shown in figure 14, but for other flow conditions, where the outflow velocity from the pipe is 30 m/s. It can be seen that as in the previous case, the pinch-effect in a two-phase round jet can satisfactorily be described by our model. As in the previous case, the intensive dispersion of particles in cross-sections is observed immediately after the concentration peak in the jet. The calculated profiles of the particle mass concentration and the velocity of the gaseous and dispersed phases in three cross-sections of the jet (at the distance of 10, 16 and 25 pipe diameters) for 23 μm particles flowing out with the mean velocity of the carrier

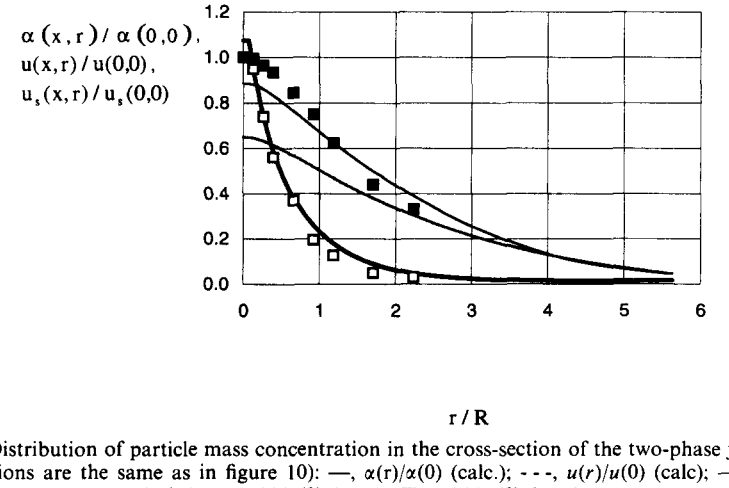

Figure 12. Distribution of particle mass concentration in the cross-section of the two-phase jet $x/D = 16$ (flow conditions are the same as in figure 10): —, $\alpha(r)/\alpha(0)$ (calc.); - - -, $u(r)/u(0)$ (calc); —, $u_s(r)/u_s(0)$ (calc.); □, $\alpha(r)/\alpha(0)$ (exp.); ■, $u_s(r)/u_s(0)$ (exp.).

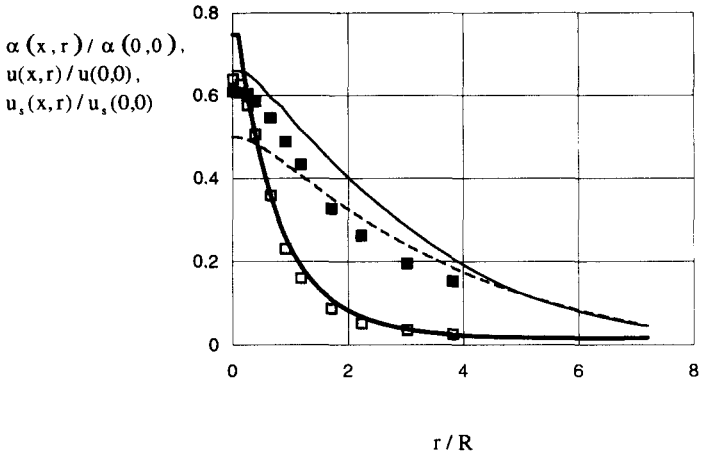

Figure 13. Distribution of particle mass concentration in the cross-section of the two-phase jet $x/D = 23$ (flow conditions are the same as in figure 10): —, $\alpha(r)/\alpha(0)$ (calc.); - - -, $u(r)/u(0)$ (calc); —, $u_s(r)/u_s(0)$ (calc.); □, $\alpha(r)/\alpha(0)$ (exp.); ■, $u_s(r)/u_s(0)$ (exp.).

fluid of 50 m/s are shown in figures 11–13. The distribution of the same parameters in the one cross-section of the jet (at the distance 16 pipe diameters), but for other mean outflow velocity of the carrier fluid of 30 m/s is given in figure 15. The numerical results have been compared with the experimental data. One can see that the profiles of particle mass concentration in the cross-section of 10 and 16 pipe diameters are narrower than the profiles in the cross-section of the jet being located further downstream at 23 pipe diameters from the outlet of the pipe. This indicates a connection between the growth of particle mass concentration along the axis of the jet and narrowing of the jet boundary downstream that speaks in favour of the existing of the pinch-effect.

The distribution of relative mass concentration along the axis for the particles of 23 μm is shown in figure 16 for the case where all the force factors (the drag force and the Magnus and Saffman lift forces), the polydispersity factor (the inter-particle collision) and the turbulence impact on the fluctuating motion of particles are included (bold curve in the figure). In this figure thin curve corresponds to the distribution of the mass concentration for the special case when the influence of the turbophoresis force is neglected. The bold dashed curve is related to the motion of fine particles when the inter-particle collision is neglected and the thin dashed curve is related to the motion when the both two factors: the turbophoresis force and inter-particle collisions are

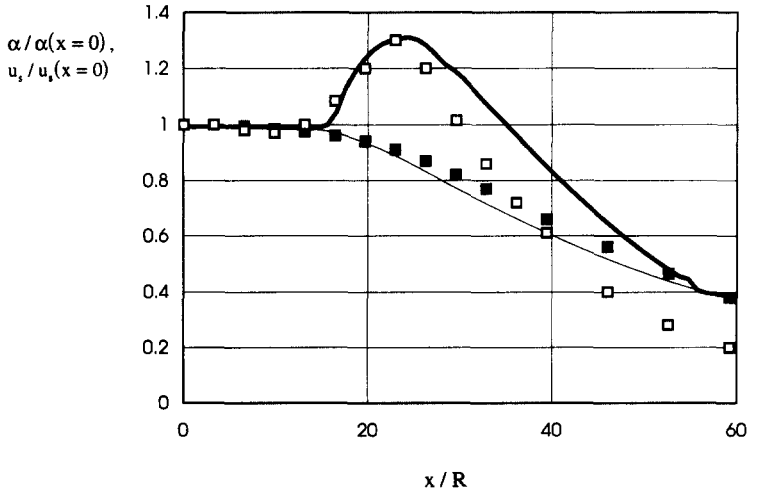

Figure 14. Distribution of particle mass concentration and the particle velocity along the axis of the two-phase jet for the following flow conditions: the mean velocity of gas at the pipe outlet $u = 30$ m/s, the pipe diameter $D = 15.2$ mm, the particle size $\delta = 23$ μm, the mass loading of 0.62 kg dust/kg air: —, $\alpha(x)/\alpha(x = 0)$ (calc.); □, $\alpha(x)/\alpha(x = 0)$ (exp.); —, $u_s(x)/u_s(x = 0)$ (calc.); ■, $u_s(x)/u_s(x = 0)$ (exp.).

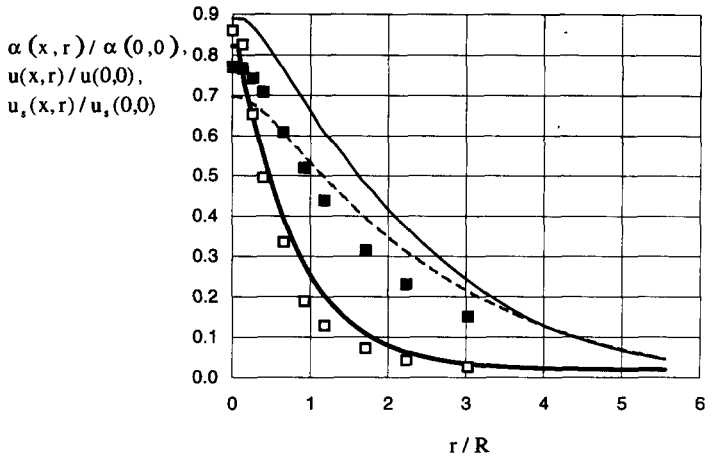

Figure 15. Distribution of particle mass concentration in the cross-section of the two-phase jet $x/D = 16$ (flow conditions are the same as in figure 14): —, $\alpha(r)/\alpha(0)$ (calc.); - - -, $u(r)/u(0)$ (calc); —, $u_s(r)/u_s(0)$ (calc.); □, $\alpha(r)/\alpha(0)$ (exp.); ■, $u_s(r)/u_s(0)$ (exp.).

neglected. But the influence of the lift forces—the Magnus and Saffman forces is still present. The perceptible growth of particle mass concentration along the jet axis in two last cases is stipulated by the substantially non-uniform distribution of particle mass concentration at the outlet of the pipe. The latter is characterized by the maximum value, which is located in the middle of the pipe radius and shows decrease towards the axis and towards the wall (figure 17). The conventional signs are the same in figures 16 and 17. Such distribution of particle mass concentration in the pipe was obtained for the same force factors as in the jet, i.e. neglecting the inter-particle collision as well as the influence of both factors together: the turbophoresis force and inter-particle collisions. As the comparison of numerically obtained profiles of mass concentration in a pipe with the experimental data for these two cases shows, the calculated distributions are substantially different from the experimental results. Due to the turbophoresis force as well as lift forces, such a distribution of the particle mass concentration in a pipe (bold and thin dashed curves in figure 17) will be re-distributed in the jet. The result is an impressive growth of the mass concentration along the jet axis (bold and thin dashed curves in figure 16). So, taking all the force factors together we can obtain the relevant distribution of particle mass concentration adequately describing the

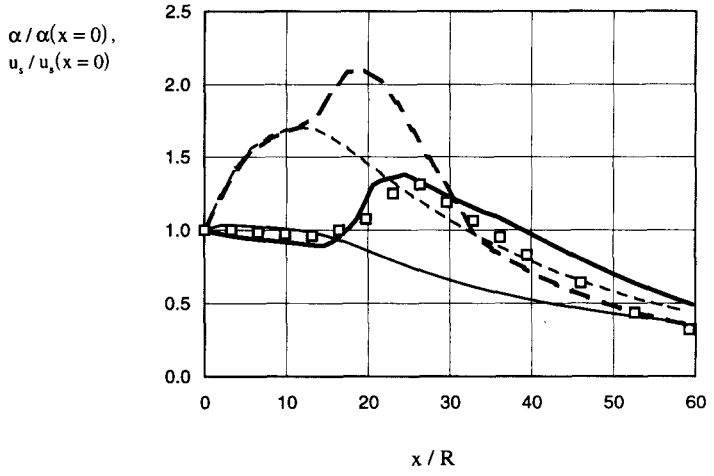

Figure 16. Distribution of particle mass concentration along the axis of the two-phase jet for the following flow conditions: the mean velocity of gas at the pipe outlet $u = 50$ m/s, the pipe diameter $D = 15.2$ mm, the particle size $\delta = 23$ μm, the mass loading of 0.62 kg dust/kg air: —, $\alpha(x)/\alpha(x = 0)$ (calc., including of all force factors); □, $\alpha(x)/\alpha(x = 0)$ (exp.); —, α (calc., neglect the influence of the turbophoresis force); - - -, α (calc., neglect the influence of inter-particle collisions); - - -, α (calc., neglect the influence of the turbophoresis force and inter-particle collision, i.e. the explicit influence of the lift forces).

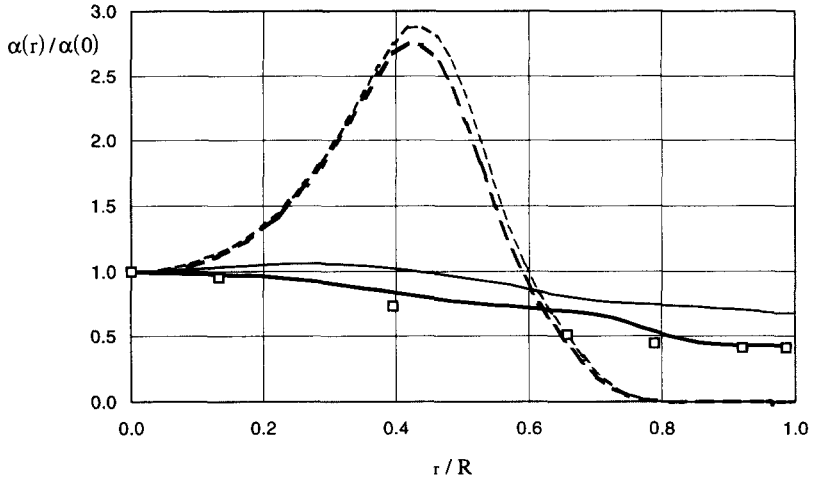

Figure 17. Distribution of particle mass concentration at the pipe outlet for different force factors (indications on the figure and flow conditions are the same as in figure 16).

pinch-effect. As the numerical calculations show, the main reason for the pinch-effect is the turbophoresis force since neglecting of this force brings to the fading of particle mass concentration along the whole length of the jet (thin curve in figure 16). This force results from by both the non-uniform distribution of the turbulent energy at the initial cross-section of the jet flow and the inter-particle collisions. These factors and the Saffman lift force can initiate the motion of particles towards the jet axis, causing the radial migration of solid particles. The turbophoresis force included in the transport equation of the momentum of the dispersed phase in the radial direction at jet expansion is

$$F_t = -\frac{\rho_s}{AA\eta}\frac{\partial}{\partial\eta}\eta(\langle v_p'^2\rangle + k_s).$$

The second term in this expression connected with the parameter k_s is the force factor initiated by the inter-particle collision, which is similar to the turbophoresis force caused by the flow turbulence. It appears from writing the expression for the normal component of the stress tensor for the dispersed phase [22]. The distribution of the pseudoviscosity diffusion coefficient originated from the inter-particle collision D_s and the coefficient of the turbulent diffusion of particles D_p in the cross-section of the pipe outlet and in the jet at 23 pipe diameters from the outlet of the pipe are shown in figures 18 and 19, respectively. These values are presented in the dimensionless form related to the coefficient of the kinematic viscosity of gas for the pipe flow and to the coefficient of the turbulent viscosity of gas for the jet flow. As it is shown, the distributions of these values

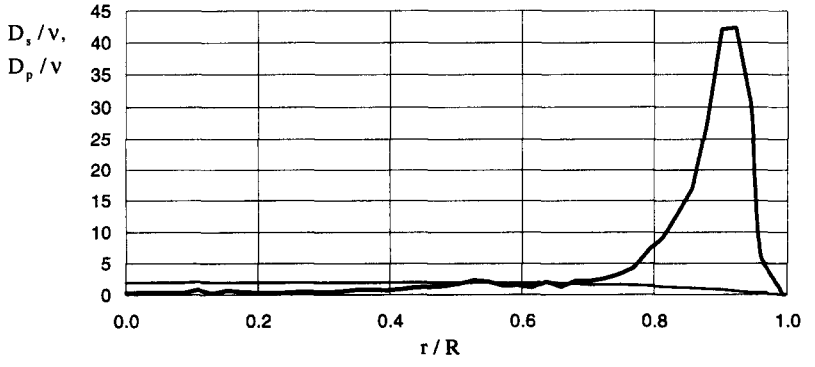

Figure 18. Distribution of the pseudoviscosity diffusion coefficient (—, D_s/v) and the coefficient of the turbulent diffusion of particles (—, D_p/v) along the radius of the pipe at its outlet (flow conditions are the same as in figure 16).

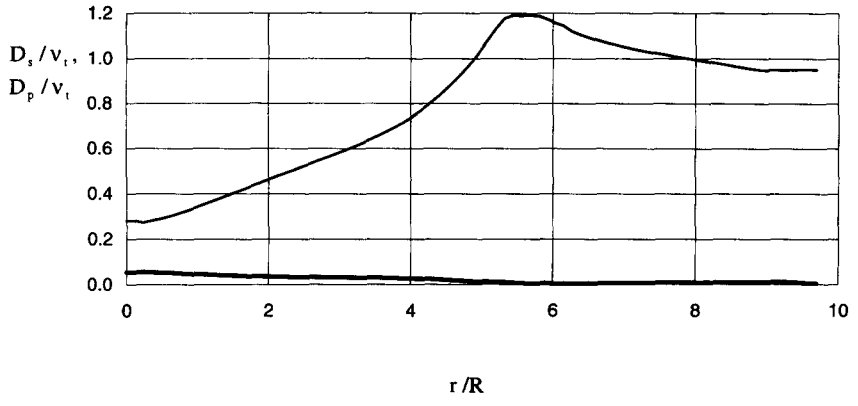

Figure 19. Distribution of pseudoviscosity diffusion coefficient (—, D_s/v_t) and the coefficient of the turbulent diffusion of particles (—, D_p/v_t) in the cross-section of the two-phase jet $x/D = 23$ (flow conditions are the same as in figure 16).

in the cross-sections of a pipe and jet flows, the influence of the inter-particle collision prevails over the turbulent diffusion of particles in the pipe near the wall. On the other hand, the influence of the turbulent diffusion of particles in the jet prevails over the inter-particle collision, increasing the influence of the turbophoresis force and resulting in the pinch-effect in the two-phase turbulent jet. The numerical calculations were also performed to describe the pinch-effect observed earlier in the experiments of Laats and Frishman (1970) when this effect was observed by using a different measurement technique (by isokinetic tubes). They defined the growth of the flow rate of particle mass as $g_s = \rho_s u_s = \rho \alpha u_s$ (here ρ_s is density of the dispersed phase) along the axis instead of the value of particle mass concentration α in the experiments of Navoznov *et al.* (1979). The numerical calculations were performed for three flow conditions: for the motion of particles of the sizes of 7, 17 and 32 μm by flowing out from the pipe with the larger diameter of 35 mm and for the mean gas outflow velocity of 50 m/s. The numerical results were compared with the experimental data obtained in our laboratory by Laats and Frishman (1970) and described the pinch-effect in that case as well.

In principal, the purpose of the given investigations is to describe the anomalies in the distribution of particle mass concentration in the pipe-jet flow. The performed calculations showed the existence of the pinch-effect in the jet and various profiles of the distribution of particle mass concentration in the cross-section of the pipe (figures 7–9). However there were the differences between the numerical and experimental results. For example, this can be seen in the distribution of concentration in the pipe (figure 4) or along the axis of the jet (figures 10, 14). In our simulation we used the semi-empirical model elaborated by Shraiber *et al.* (1990) where we could describe the turbulent diffusion of particles. Unfortunately, we could not, for example, adequately describe the distribution of concentration in the development stages of the jet by this model. This is due to the selection of numerical constants in the semi-empirical model of Shraiber *et al.* (1990). The further improvements can be the following:

(1) verification of the empirical constants of the model (Shraiber *et al.* 1990), or using other models describing the turbulent diffusion and two-way coupling effects for the motion of fine particles in the pipe-jet flow;

(2) more accurate calculations of the inter-particle collision (introducing a greater number of particle fractions), which can show the stronger effect and thus give the better description of experimental data.

7. CONCLUSION

(1) The results of the numerical simulation of the pinch-effect for the distribution of the solid admixture concentration in the two-phase round submerged jet carrying fine solid particles discovered at the beginning of 1970s and not been satisfactorily explained are given now.

(2) Since the reasons resulting in the distribution anomalies of the particle mass concentration have not been known, the presented model takes into account the influence of all factors, which can cause such distributions in real dispersed flows: the polydispersity, the two-way coupling processes, the Magnus and Saffman lift forces, the turbophoresis force and the particle interaction with the wall and with each other.

(3) Special attention was paid to the influence of the admixture polydispersity since the real manufactured powders are polydispersed. The model of the closure of transport equations of the dispersed phase based on the inter-particle collisions was elaborated. It is indicated that with neglecting the inter-particle collisions and the influence of the turbophoresis force, the anomalous distributions of particle mass concentration in the pipe and jet flows cannot be described.

(4) By the given model the motion in a two-phase pipe-jet flow was calculated. This allowed to set the initial boundary conditions to the two-phase jet, including the initial distribution of the parameters, which do not respond to the direct experimental measurements properly.

(5) The calculation results have been compared with the experimental data obtained by the authors for various flows, using different experimental techniques. The numerical results describe satisfactorily the parameters of both phases in a pipe and a jet, including the anomalous distributions.

Acknowledgements—The given work was supported by a Grant of the Joint Program of the Government of Estonia and the International Science Foundation No. LK 6100. The authors are grateful to Mr Tisler for his help in designing and typing this manuscript.

REFERENCES

Abramovich, G. N. (1970) The effect of an admixture of solid particles or droplets on the structure of turbulent gas jet. *Soviet Phys. Dokl.* **190,** 1052–1055 (in Russian).

Abramovich, G. N., Bazhanov, V. I. and Girshovich, T. A. (1972) Turbulent jet with heavy admixtures. *Notices of the Academy of Sciences of the USSR, Series Mekhanika zhydkosti i gaza* **6,** 41–49 (in Russian).

Abramovich, G. N., Girshovich, T. A., Krasheninnikov, S. Yu., Sekundov, A. N. and Smirnova, I. P. (1984) *Theory of Turbulent Jets*. Nauka, Moscow (in Russian).

Babukha, G. L. and Shraiber, A. A. (1972) *Interaction of Particles of Polydispersive Material in Two-phase Flows*. Naukova Dumka, Kiev (in Russian).

Brailovskaja, I. Yu. and Chudov, L. A. (1962) Solution of the equations of the boundary layer by the difference method. In *Numerical Methods and Programming*, Part 1, pp. 167–182.

Chapman, S. and Cowling, T. G. (1970) *The Mathematical Theory of Non-uniform Gases*, 3rd edn. Cambridge University Press, Cambridge.

Crowe, C. T., Sharma, M. P. and Stock, D. E. (1977) The particle-source-in-cell (PSI-CELL) for gas droplet flows. *J. Fluids Engr.* **99,** 325–332.

Durst, F. and Rastogi, A. K. (1977) Calculations of turbulent boundary layer flows with drag reducing polymer additives. *Phys. Fluids* **20,** 1975–1985.

Elghobashi, S. E. and Abou-Arab, T. W. (1983) A two-equation turbulence model for two-phase flows. *Phys. Fluids* **26,** 931–938.

Fletcher, R. D. (1967) Suspension stratification in the atmosphere. *Phys. Fluids Suppl.* **9,** 223–385.

Fortier, A. (1967) *Mechanique des suspensions*. Masson et Cie, Paris.

Frishman, F., Kartushinsky, A. and Shcheglov, I. (1993) Diffusion anomalies of solid particles in turbulent flows. *Proc. Estonian Acad. Sci. Phys. Math.* **42,** 242–250.

Gorbis, Z. R. Spokoinyi, F. E. (1977) Physical model and mathematical description of the process of fine particle motion in turbulent gas suspension flow. *Teplofizika Vysokikh Temperatur* **15,** 399–408 (in Russian).

He, J. and Simonin, O. (1993) Non-equilibrium prediction of the particle-phase stress tensor in vertical pneumatic conveying. *EDF Report HE*-44, Vol. 15, pp. 1–24.

Hetsroni, G. and Sokolov, M. (1971) Distribution of mass, velocity and intensity of turbulence in a two-phase turbulent jet. *Trans. ASME J. Appl. Mech.* **38,** 315–327.

Hussainov, M., Kartushinsky, A., Mulgi, A. and Rudi, U. (1995) Experimental and theoretical study of the distribution of mass concentration of solid particles in the two-phase laminar boundary layer on a flat plate. *Int. J. Multiphase Flow*, **21,** 1141–1161.

Hussainov, M., Kartushinsky, A., Mulgi, A. and Rudi, U. (1996) Gas–solid flow with the slip velocity of particles in a horizontal channel. *J. Aerosol Sci.* **27,** 41–59.

Jenkins, J. T. and Savage, S. B. (1983) A theory for the rapid flow of identical, smooth, nearly elastic, spherical particles. *J. Fluid Mech.* **130,** 187–202.

Kartushinsky, A. I. (1984) Transfer of inertial admixture in two-phase turbulent jet. *Izv. Akad. Nauk SSSR Mekh. Zhidk, Gasa* **4,** 36–41 (in Russian).

Kohnen, G., Rüger, M. and Sommerfeld, M. (1994) Convergence behavior for numerical calculations by the Euler/Lagrange method for strongly coupled phases. *International Symposium Numerical Methods for Multiphase Flows*, ASME FED Vol. 185, pp. 191–202.

Kravtsov, M. V. (1968) Drag to the free steady motion of a sphere in the viscous medium. *J. Engng Phys* **XV,** 464–470 (in Russian).

Kramer, T. J. and Depew, C. A. (1972) Experimentally determined mean flow characteristics of gas-solid suspensions. *Transactions of the ASME, Journal of Basic Engineering, Ser. D* **2,** 254–262.

Krasheninnikov, S. Yu. (1972) Of calculation of the axisymmetrical swirling turbulent jets. *Izv. Akad. Nauk SSSR Mekh. Zidk, Gasa* **3,** 71–80 (in Russian).

Kulick, J. D., Fessler, J. R. and Eaton, J. K. (1994) Particle response and turbulence modification in fully developed channel flow. *Journal Fluid Mechanics* **277,** 109–134.

Laats, M. K. and Frishman, F. M. (1970) Assumptions used for the calculation of the two-phase turbulent jet. *Izv. Akad. Nauk SSSR Mekh. Zhidk, Gasa* **2,** 186–191.

Laats, M. K. and Frishman, F. M. (1973) The development of the methods and investigation of turbulence intensity at the axis of two-phase turbulent jet. *Izv. Akad. Nauk SSSR Mekh. Zhidk, Gasa* **2,** 153–157.

Lee, S. L. and Durst, F. (1982) On the motion of particles in turbulent duct flow. *Int. J. Multiphase Flow* **8,** 125–146.

Louge, M. Y., Mastorakos, E. and Jenkins, J. T. (1991) The role of particle collisions in pneumatic transport. *Journal Fluid Mechanics* **231,** 345–359.

Marble, F. E. (1964) Mechanism of particle collision in one-dimensional dynamics of gas–particle admixture. *Phys. Fluids* **7,** 1270–1282.

Mednikov, Ye. P. (1981) *Turbulent Transfer and Precipitation of Aerosols*. Nauka, Moscow (in Russian).

Mei, R. (1992) An approximate expression for the shear lift force on a spherical particle at finite Reynolds number. *Int. J. Multiphase Flow* **18,** 145–147.

Melville, W. K. and Bray, K. N. C. (1979) A model of the two-phase turbulent jet. *Int. J. Heat Mass Transfer* **22,** 647–656.

Melville, W. K. and Bray, K. N. C. (1979) The two-phase turbulent jet. *Int. J. Heat Mass Transfer* **22,** 279–287.

Navoznov, S. I., Pavel'ev, A. A., Mulgi, A. S. and Laats, M. K. (1979) Effect of initial slip on admixture dispersion in two-phase jet. In *Turbulent Two-phase Flows*, pp. 149–157. Tallinn, Moscow (in Russian).

Nigmatulin, R. I. (1990) *Dynamics of Multiphase Media*, Vol. 1. Hemisphere, New York.

Patankar, S. (1980) *Numerical Heat Transfer and Fluid Flow*. Hemisphere, New York.

Rubinow, S. I. and Keller, J. B. (1961) The transverse force on a spinning sphere moving in a viscous fluid. *J. Fluid Mech.* **11,** 447–459.

Shraiber, A. A., Yatsenko, V. P., Gavin, L. B. and Naumov, V. A. (1990) *Turbulent Flows in Gas Suspensions*. Hemisphere, New York.

Sommerfeld, M. (1992) Modelling of particle-wall collisions in confined gas–particle flows. *Int. J. Multiphase Flow* **18,** 905–926.

Sommerfeld, M. and Zivkovic, G. (1992) Recent advances in the numerical simulation of pneumatic conveying through pipe systems. In *Computational Methods in Applied Science*, pp. 201–212. Elsevier, Amsterdam.

Sommerfeld, M. (1995) The importance of inter-particle collisions in horizontal gas–solid channel flows. Gas–Particle Flows. *ASME, FED* **228,** 335–345.

Trushin, G. I. and Lipatov, N. N. (1963) The probability of collision of the suspended particles in their orientated motion. *Izv. Vizshih Uchebnih Zavedeni. Pischevaya, Technologiya* **5,** 110–114 (in Russian).

Tsuji, Y., Morikava, Y. and Shiomi, H. (1984) LDV measurements of an air–solid two-phase flow in a vertical pipe. *J. Fluid Mech.* **139,** 417–434.

Vasilkov, A. I. (1976) Calculation of turbulent two-phase isobar jet. *Izv. Akad. Nauk SSSR Mekh. Zidk, Gasa* **5,** 57–63 (in Russian).

Yarin, L. P. and Hetsroni, G. (1994a) Turbulence intensity in dilute two-phase flows—1. Effect of particle-size distribution on the turbulence of the carrier fluid. *Int. J. Multiphase Flow* **20,** 1–15.

Yarin, L. P. and Hetsroni, G. (1994b) Turbulence intensity in dilute two-phase flows—3. The particles–turbulence interaction in dilute two-phase flow. *Int. J. Multiphase Flow* **20,** 27–44.

APPENDIX A

The velocity differences for the translational and angular velocities of the colliding two particles written in vector form are the following:

$$\mathbf{V}_1' - \mathbf{V}_1 = \beta_{21}\left\{(1-k_{np})[\mathbf{e}\cdot(\mathbf{V}_2-\mathbf{V}_1)]\mathbf{e} + \frac{(1-k_{tp})\xi}{(1+\xi)}\mathbf{e} \times \left[(\mathbf{V}_2-\mathbf{V}_1)\times\mathbf{e} - \frac{(\delta_1\boldsymbol{\omega}_1+\delta_2\boldsymbol{\omega}_2)}{2}\right]\right\}, \quad [A1]$$

$$\mathbf{V}_2' - \mathbf{V}_2 = -\beta_{12}\left\{(1-k_{np})[\mathbf{e}\cdot(\mathbf{V}_2-\mathbf{V}_1)]\mathbf{e} + \frac{(1-k_{tp})\xi}{(1+\xi)}\mathbf{e} \times \left[(\mathbf{V}_2-\mathbf{V}_1)\times\mathbf{e} - \frac{(\delta_1\boldsymbol{\omega}_1+\delta_2\boldsymbol{\omega}_2)}{2}\right]\right\}, \quad [A2]$$

$$\boldsymbol{\omega}_1' - \boldsymbol{\omega}_1 = -\beta_{21}\frac{(1-k_{tp})}{(1+\xi)}\left\{\frac{2}{\delta_1}\mathbf{e}\times(\mathbf{V}_2-\mathbf{V}_1) + \boldsymbol{\omega}_1 + \frac{\delta_2}{\delta_1}\boldsymbol{\omega}_2 - \left(\mathbf{e}\cdot\boldsymbol{\omega}_1 + \frac{\delta_2}{\delta_1}\mathbf{e}\cdot\boldsymbol{\omega}_2\right)\right\}, \quad [A3]$$

$$\boldsymbol{\omega}_2' - \boldsymbol{\omega}_2 = -\beta_{12}\frac{(1-k_{tp})}{(1+\xi)}\left\{\frac{2}{\delta_2}\mathbf{e}\times(\mathbf{V}_2-\mathbf{V}_1) + \boldsymbol{\omega}_2 + \frac{\delta_1}{\delta_2}\boldsymbol{\omega}_1 - \left(\mathbf{e}\cdot\boldsymbol{\omega}_2 + \frac{\delta_1}{\delta_2}\mathbf{e}\cdot\boldsymbol{\omega}_1\right)\right\}. \quad [A4]$$

The expressions [A1]–[A4] for this particular case of two colliding particles are the generalized form of Chapman and Cowling (1970) and presented with taking into account the restitution and friction by Babukha and Shraiber (1972).

The velocity differences presented in the Cartesian coordinates for the axial and radial velocity components and for the angular velocity component are the following:

$$u_{21}' - u_1 = \beta_{21}\cos\gamma_1\left\{(a-c\chi^2)(V_2\cos\varphi - V_1 - V_2\sin\varphi\,\mathrm{tg}\gamma_1) - c\chi\sqrt{1-\chi^2}\sin\theta \times[(V_2\cos\varphi - V_1)\mathrm{tg}\gamma_1 + V_2\sin\varphi] - \frac{d_{12}}{\sqrt{V_1^2+V_2^2-2V_1V_2\cos\varphi}}[\sqrt{1-\chi^2}((V_2\cos\varphi - V_1)\mathrm{tg}\gamma_1 + V_2\sin\varphi) + \chi\sin\theta(V_2\cos\varphi - V_1 - V_2\sin\varphi\,\mathrm{tg}\gamma_1)]\right\}, \quad [A5]$$

$$v'_{21} - v_1 = \beta_{21}\cos\gamma_1\Big\{(a - c\chi^2)((V_2\cos\varphi - V_1)\mathrm{tg}\gamma_1 + V_2\sin\varphi) - c\chi\sqrt{1-\chi^2}\sin\theta$$

$$\times(V_2\cos\varphi - V_1 - V_2\sin\varphi\,\mathrm{tg}\gamma_1) + \frac{d_{12}}{\sqrt{V_1^2 + V_2^2 - 2V_1V_2\cos\varphi}}[\sqrt{1-\chi^2}(V_2\cos\varphi - V_1$$

$$- V_2\sin\varphi\,\mathrm{tg}\gamma_1) - \chi\sin\theta((V_2\cos\varphi - V_1)\mathrm{tg}\gamma_1 + V_2\sin\varphi)]\Big\}, \qquad [A6]$$

$$u'_{12} - u_2 = -\beta_{12}\cos\gamma_1\Big\{(a - c\chi^2)(V_2\cos\varphi - V_1 - V_2\sin\varphi\,\mathrm{tg}\gamma_1) - c\chi\sqrt{1-\chi^2}\sin\theta$$

$$\times[(V_2\cos\varphi - V_1)\mathrm{tg}\gamma_1 + V_2\sin\varphi] - \frac{d_{12}}{\sqrt{V_1^2 + V_2^2 - 2V_1V_2\cos\varphi}}[\sqrt{1-\chi^2}((V_2\cos\varphi$$

$$- V_1)\mathrm{tg}\gamma_1 + V_2\sin\varphi) + \chi\sin\theta(V_2\cos\varphi - V_1 - V_2\sin\varphi\,\mathrm{tg}\gamma_1)]\Big\}, \qquad [A7]$$

$$v'_{12} - v_2 = -\beta_{12}\cos\gamma_1\Big\{(a - c\chi^2)((V_2\cos\varphi - V_1)\mathrm{tg}\gamma_1 + V_2\sin\varphi) - c\chi\sqrt{1-\chi^2}\sin\theta$$

$$\times[(V_2\cos\varphi - V_1 - V_2\sin\varphi\,\mathrm{tg}\gamma_1) + \frac{d_{12}}{\sqrt{V_1^2 + V_2^2 - 2V_1V_2\cos\varphi}}[\sqrt{1-\chi^2}(V_2\cos\varphi - V_1$$

$$- V_2\sin\varphi\,\mathrm{tg}\gamma_1) - \chi\sin\theta((V_2\cos\varphi - V_1)\mathrm{tg}\gamma_1 + V_2\sin\varphi)]\Big\}, \qquad [A8]$$

$$\omega'_{21} - \omega_1 = \frac{2\beta_{21}b}{\xi\delta_1}\left[\chi\sqrt{V_1^2 + V_2^2 - 2V_1V_2\cos\varphi}\sin\theta - \frac{d_{12}}{b}(1 - \chi^2\cos^2\theta)\right], \qquad [A9]$$

$$\omega'_{12} - \omega_2 = \frac{2\beta_{12}b}{\xi\delta_2}\left[\chi\sqrt{V_1^2 + V_2^2 - 2V_1V_2\cos\varphi}\sin\theta - \frac{d_{12}}{b}(1 - \chi^2\cos^2\theta)\right], \qquad [A10]$$

where the coefficients are

$$a = 1 - k_{np}, \quad b = \frac{(1 - k_{tp})\xi}{(1 + \xi)}, \quad c = a - b, \quad d_{12} = \frac{b(\delta_1\omega_1 + \delta_2\omega_2)}{2}$$

and the angle is

$$\gamma_1 = \mathrm{arctg}\left(\frac{v_1}{\sqrt{u_1^2 + v_1^2}}\right).$$

APPENDIX B

In the case of the binary collisions of particles of three sizes the coefficients are determined as following:

$$\bar{P}_{ij} = (V_i + V_j)^2\Big\{\frac{1}{2}\left(\frac{a+b}{2}\right)^2\Big[\mathrm{tg}2\gamma_i\left(1 - \frac{k_{ij}^2}{2}\left(1 + \frac{\sin\varphi_{ij}}{\varphi_{ij}}\right) - \frac{V_j}{V_i}\frac{k_{ij}^2}{4}\left(1 - \frac{\sin 2\varphi_{ij}}{2\varphi_{ij}}\right)\right) - k_{ij}^2\frac{\sin^2\frac{\varphi_{ij}}{2}}{\varphi_{ij}}$$

$$\times\left(1-\frac{V_j}{V_i}\cos^2\frac{\varphi_{ij}}{2}\right)\Bigg]+b\frac{(2a+3b)}{15\varphi_{ij}}\left(\frac{\delta_i\omega_i+\delta_j\omega_j}{V_i+V_j}\right)\Bigg[\left(1-\frac{2V_j(2-k_{ij}^2)}{3V_ik_{ij}^2}\right)\int_0^{\varphi_{ij}}\sqrt{1-k_{ij}^2\cos^2\frac{\varphi}{2}}\,\mathrm{d}\varphi+\frac{4V_j}{3V_i}$$

$$\times\frac{(1-k_{ij}^2)}{k_{ij}^2}\int_0^{\varphi_{ij}}\frac{\mathrm{d}\varphi}{\sqrt{1-k_{ij}^2\cos^2\frac{\varphi}{2}}}-\frac{2V_j\sin\varphi_{ij}}{3V_i}\sqrt{1-k_{ij}^2\cos^2\frac{\varphi_{ij}}{2}}-\left(1+\frac{V_j}{V_i}\right)\left(1-\sqrt{\frac{1-k_{ij}^2\cos^2\frac{\varphi_{ij}}{2}}{1-k_{ij}^2}}\right)$$

$$\times\sqrt{1-k_{ij}^2}\left(1-\frac{V_j}{V_i}+\left(1+\frac{V_j}{V_i}\right)\frac{(1-k_{ij}^2)}{3}\left(1+\sqrt{\frac{1-k_{ij}^2\cos^2\frac{\varphi_{ij}}{2}}{1-k_{ij}^2}+\frac{1-k_{ij}^2\cos^2\frac{\varphi_{ij}}{2}}{1-k_{ij}^2}}\right)\mathrm{tg}2\gamma_i\right)\Bigg]$$

$$+\frac{b^2}{16}\left(\frac{\delta_i\omega_i+\delta_j\omega_j}{V_i+V_j}\right)^2\Bigg[\Bigg(\Bigg(\frac{V_j}{V_i}\left(\frac{1-k_{ij}^2}{k_{ij}^2}+\frac{1}{2}\left(1+\frac{\sin\varphi_{ij}}{\varphi_{ij}}\right)-\frac{2\sqrt{1-k_{ij}^2}}{\varphi_{ij}k_{ij}^2}\operatorname{arctg}\left(\frac{\mathrm{tg}\frac{\varphi_{ij}}{2}}{\sqrt{1-k_{ij}^2}}\right)\right)-\frac{1}{2}\Bigg)\mathrm{tg}2\gamma_i$$

$$+\frac{1}{\varphi_{ij}}\left(\frac{V_j}{V_i}\sin^2\frac{\varphi_{ij}}{2}+\frac{1}{4}\left(1-\frac{V_j^2}{V_i^2}\right)\ln\left(\frac{1-k_{ij}^2\cos^2\frac{\varphi_{ij}}{2}}{1-k_{ij}^2}\right)\right)\Bigg]\Bigg\}\cos 2\gamma_i, \qquad \text{[B1]}$$

$$\bar{R}_{ij}=(V_i+V_j)^2\Bigg\{\left(\frac{1}{3}\left(\frac{a-b}{2}\right)^2+\left(\frac{a+b}{2}\right)^2\sin^2\gamma_i\right)\left(1-\frac{k_{ij}^2}{2}\left(1+\frac{\sin\varphi_{ij}}{\varphi_{ij}}\right)\right)+\left(\frac{a+b}{2}\right)^2\frac{k_{ij}^2}{2}\cos 2\gamma_i$$

$$\times\left(\frac{V_j}{4V_i}\left(1-\frac{\sin 2\varphi_{ij}}{2\varphi_{ij}}\right)-\mathrm{tg}2\gamma_i\frac{\sin^2\frac{\varphi_{ij}}{2}}{\varphi_{ij}}\left(1-\frac{V_j}{V_i}\cos^2\frac{\varphi_{ij}}{2}\right)\right)+b\frac{(2a+3b)}{15\varphi_{ij}}\left(\frac{\delta_i\omega_i+\delta_j\omega_j}{V_i+V_j}\right)\Bigg[\left(1+\frac{V_j}{V_i}\right)$$

$$\times\left(1-\sqrt{\frac{1-k_{ij}^2\cos^2\frac{\varphi_{ij}}{2}}{1-k_{ij}^2}}\right)\left(1-\frac{V_j}{V_i}+\left(1-\frac{V_j}{V_i}\right)\frac{(1-k_{ij}^2)}{3}\left(1+\sqrt{\frac{1-k_{ij}^2\cos^2\frac{\varphi_{ij}}{2}}{1-k_{ij}^2}+\frac{1-k_{ij}^2\cos^2\frac{\varphi_{ij}}{2}}{1-k_{ij}^2}}\right)\right)$$

$$\times\sqrt{1-k_{ij}^2}+\left(\left(1-\frac{2V_j(2-k_{ij}^2)}{3V_ik_{ij}^2}\right)\int_0^{\varphi_{ij}}\sqrt{1-k_{ij}^2\cos^2\frac{\varphi}{2}}\,\mathrm{d}\varphi+\frac{4V_j(1-k_{ij}^2)}{3V_ik_{ij}^2}\int_0^{\varphi_{ij}}\frac{\mathrm{d}\varphi}{\sqrt{1-k_{ij}^2\cos^2\frac{\varphi}{2}}}-\frac{2V_j}{3V_i}\right.$$

$$\left.\times\sin\varphi_{ij}\sqrt{1-k_{ij}^2\cos^2\frac{\varphi_{ij}}{2}}\right)\mathrm{tg}2\gamma_i\Bigg]+\frac{b^2}{16}\left(\frac{\delta_i\omega_i+\delta_j\omega_j}{V_i+V_j}\right)^2\Bigg[1+\cos^2\gamma_i-\cos 2\gamma_i\Bigg[\frac{V_j}{V_i}\left(\frac{1-k_{ij}^2}{k_{ij}^2}\right.$$

$$+\frac{1}{2}\left(1+\frac{\sin\varphi_{ij}}{\varphi_{ij}}\right)-\frac{2\sqrt{1-k_{ij}^2}}{\varphi_{ij}k_{ij}^2}\operatorname{arctg}\left(\frac{\mathrm{tg}\frac{\varphi_{ij}}{2}}{\sqrt{1-k_{ij}^2}}\right)\Bigg)-\left(\frac{V_j}{V_i}\sin^2\frac{\varphi_{ij}}{2}+\frac{1}{4}\left(1-\frac{V_j^2}{V_i^2}\right)\ln\left(\frac{1-k_{ij}^2\cos^2\frac{\varphi_{ij}}{2}}{1-k_{ij}^2}\right)\right)$$

$$\left.\times\frac{\mathrm{tg}2\gamma_i}{\varphi_{ij}}\Bigg]\Bigg]\Bigg\}, \qquad \text{[B2]}$$

$$\bar{S} = \frac{b}{15\zeta}(V_i - V_j)^2 \left\{ 4(a-b)\left[\frac{k_{ij}}{3}\sqrt{\frac{V_j}{V_i}}\left(\sin\varphi_{ij}\sqrt{1-k_{ij}^2\cos^2\frac{\varphi_{ij}}{2}} + \frac{(1-k_{ij}^2)}{k_{ij}^2}\int_0^{\varphi_{ij}} \frac{d\varphi}{\sqrt{1-k_{ij}^2\cos^2\frac{\varphi}{2}}}\right)\right.\right.$$

$$\left.\left. -\left(1 - \frac{(2k_{ij}^2-1)}{3k_{ij}}\sqrt{\frac{V_j}{V_i}}\right)\int_0^{\varphi_{ij}}\sqrt{1-k_{ij}^2\cos^2\frac{\varphi}{2}}\,d\varphi + \mathrm{tg}\gamma_i\left(1+\frac{V_j}{V_i}\right)\frac{(1-k_{ij}^2)^{1.5}}{3}\left(1-\left(\frac{1-k_{ij}^2\cos^2\frac{\varphi_{ij}}{2}}{1-k_{ij}^2}\right)^{1.5}\right)\right]\right.$$

$$+\frac{5}{2}\frac{(5a+7b)}{\left(1+\frac{V_j}{V_i}\right)}\left(\frac{\delta_i\omega_i+\delta_j\omega_j}{V_i+V_j}\right)\left(\left(1-\frac{V_j}{V_i}\frac{\sin\varphi_{ij}}{\varphi_{ij}}\right)\varphi_{ij}\frac{\mathrm{tg}\gamma_i}{2} - \frac{V_j}{V_i}\sin^2\frac{\varphi_{ij}}{2}\right) + 2b\left(\frac{\delta_i\omega_i+\delta_j\omega_j}{V_i+V_j}\right)^2$$

$$\times\left[\left(1-\frac{V_j}{V_i}\right)\int_0^{\varphi_{ij}}\frac{d\varphi}{\sqrt{1-k_{ij}^2\cos^2\frac{\varphi}{2}}} + \left(1+\frac{V_j}{V_i}\right)\left(\int_0^{\varphi_{ij}}\sqrt{1-k_{ij}^2\cos^2\frac{\varphi}{2}}\,d\varphi\right.\right.$$

$$\left.\left. -\sqrt{1-k_{ij}^2}\left(1-\sqrt{\frac{1-k_{ij}^2\cos^2\frac{\varphi_{ij}}{2}}{1-k_{ij}^2}}\right)2\mathrm{tg}\gamma_i\right)\right]\Bigg\}\frac{\cos\gamma_i}{\varphi_{ij}}, \quad \text{[B3]}$$

$$\bar{T}_{ij} = (V_i+V_j)^2\left[\frac{1}{3}\left(\left(\frac{a+b}{2}\right)^2 + a^2 + b^2\right)\left(1-\frac{k_{ij}^2}{2}\left(1+\frac{\sin\varphi_{ij}}{\varphi_{ij}}\right)\right) + \frac{3b^2}{16}\left(\frac{\delta_i\omega_i+\delta_j\omega_j}{V_i+V_j}\right)^2\right], \quad \text{[B4]}$$

where $\bar{P}_{ij} = \bar{P}_{ji}$, $\bar{R}_{ij} = \bar{R}_{ji}$, $\bar{S}_{ij} = \bar{S}_{ji}$, $\bar{T}_{ij} = \bar{T}_{ji}$.

The stress tensor components are determined as:

$$\langle(u'_{sij}-u_{si})(v'_{sij}-v_{si})\rangle|_{\theta,\chi,\varphi} = \beta_{ij}^2\bar{P}_{ij}, \quad \langle(v'_{sij}-v_{si})^2\rangle|_{\theta,\chi,\varphi} = \beta_{ij}^2\bar{R}_{ij}, \quad \langle(\omega'_{sij}-\omega_{si})(v'_{sij}-v_{si})\rangle|_{\theta,\chi,\varphi} = \beta_{ij}^2\frac{\bar{S}_{ij}}{\delta_i},$$

$$\langle[(u'_{sij}-u_{si})^2 + (v'_{sij}-v_{si})^2]\rangle = \beta_{ji}^2\bar{T}_{ij},$$

where $i = 1, 3$; $j = 1, 3$ and $i \neq j$.

APPENDIX C

$$X_{ij}^1 = \left\{ g_1[(A_{ij}-C_{ij})\sin 2\gamma_i - B_{ij}\cos 2\gamma_i] + g_2R_{ij}(D_{ij}\cos 2\gamma_i - F_{ij}\sin 2\gamma_i) + g_3R_{ij}^2\left[\sin 2\gamma_i \times\left(G_{ij}-\frac{Q_{ij}}{2}\right) + H_{ij}\cos 2\gamma_i\right]\right\}, \quad \text{[C1]}$$

$$X_{ij}^2 = \{g_4A_{ij} + g_1(2A_{ij}\sin^2\gamma_i - B_{ij}\sin 2\gamma_i - C_{ij}\cos 2\gamma_i) + g_2R_{ij}(D_{ij}\sin 2\gamma_i + F_{ij}\cos 2\gamma_i) + g_3R_{ij}^2[Q_{ij}(1+\cos^2\gamma_i) - G_{ij}\cos 2\gamma_i + H_{ij}\sin\gamma_i]\}, \quad \text{[C2]}$$

$$X_{ij}^3 = \{g_5(L_{ij} + M_{ij}\mathrm{tg}\gamma_i) + g_6R_{ij}(N_{ij}\mathrm{tg}\gamma_i - O_{ij}) + g_7R_{ij}^2(P_{ij} - T_{ij}\mathrm{tg}\gamma_i)\}, \quad \text{[C3]}$$

$$X_{ij}^4 = g_8A_{ij} + g_9R_{ij}^2Q_{ij}, \quad \text{[C4]}$$

$$Y_{ij} = g_8 \frac{A_{ij}}{Q_{ij}} + g_9 R_{ij}^2 \qquad [C5]$$

and $X_{ij}^k = X_{ji}^k$; here the indices are determined as follows: $i = 1, 3$; $j = 1, 3$ and $i \neq j$.

The coefficients are determined as follows:

$$g_1 = \frac{1}{2}\left(\frac{a+b}{2}\right)^2, \quad g_2 = \frac{(2a+3b)b}{15}, \quad g_3 = \frac{b^2}{16}, \quad g_4 = \frac{1}{3}\left(\frac{a-b}{2}\right)^2, \quad g_5 = 2b(a-b),$$

$$g_6 = \frac{5}{4}b(5a+7b), \quad g_7 = b^2, \quad g_8 = \frac{1}{3}\left[\left(\frac{a+b}{2}\right)^2 + a^2 + b^2\right], \quad g_9 = \frac{3b^2}{16},$$

and other coefficients are determined as follows:

$$A_{ij} = \frac{\varphi_{ij}}{E^{ij}}\left(1 - \frac{k_{ij}^2}{2}\left(1 + \frac{\sin\varphi_{ij}}{\varphi_{ij}}\right)\right), \qquad [C6]$$

$$B_{ij} = \frac{k_{ij}^2 \sin^2\frac{\varphi_{ij}}{2}}{E^{ij}}\left(1 - \frac{V_j}{V_i}\cos^2\frac{\varphi_{ij}}{2}\right), \qquad [C7]$$

$$C_{ij} = \frac{k_{ij}^2}{4}\frac{V_j}{V_i}\frac{\varphi_{ij}}{E^{ij}}\left(1 - \frac{\sin 2\varphi_{ij}}{2\varphi_{ij}}\right), \qquad [C8]$$

$$D_{ij} = 1 - \frac{2V_j(2-k_{ij}^2)}{2V_i k_{ij}^2} + \frac{4V_j(1-k_{ij}^2)K^{ij}}{3V_i k_{ij}^2 E^{ij}} - \frac{2V_j \sin\varphi_{ij}}{3V_i E^{ij}}\sqrt{1 - k_{ij}^2\cos^2\frac{\varphi_{ij}}{2}}, \qquad [C9]$$

$$F_{ij} = \frac{\left(1+\frac{V_j}{V_i}\right)\sqrt{1-k_{ij}^2}}{E^{ij}}\left(1 - \sqrt{\frac{1-k_{ij}^2\cos^2\frac{\varphi_{ij}}{2}}{1-k_{ij}^2}}\right)\left(1 - \frac{V_j}{V_i} + \left(1+\frac{V_j}{V_i}\right)\frac{\sqrt{1-k_{ij}^2}}{3}\left(1 + \sqrt{\frac{1-k_{ij}^2\cos^2\frac{\varphi_{ij}}{2}}{1-k_{ij}^2}}\right.\right.$$

$$\left.\left. + \frac{1-k_{ij}^2\cos^2\frac{\varphi_{ij}}{2}}{1-k_{ij}^2}\right)\right), \qquad [C10]$$

$$G_{ij} = \frac{V_j\varphi_{ij}}{V_i E^{ij}}\left(\frac{1-k_{ij}^2}{k_{ij}^2} + \frac{1}{2}\left(1 + \frac{\sin\varphi_{ij}}{\varphi_{ij}}\right) - \frac{2\sqrt{1-k_{ij}^2}}{\varphi_{ij}k_{ij}^2}\operatorname{arctg}\left(\frac{\operatorname{tg}\frac{\varphi_{ij}}{2}}{\sqrt{1-k_{ij}^2}}\right)\right), \qquad [C11]$$

$$H_{ij} = \left(\frac{V_j}{V_i}\sin^2\frac{\varphi_{ij}}{2} + \frac{1}{4}\left(1 - \frac{V_j^2}{V_i^2}\right)\ln\left(\frac{1-k_{ij}^2\cos^2\frac{\varphi_{ij}}{2}}{1-k_{ij}^2}\right)\right)\frac{1}{E^{ij}}, \qquad [C12]$$

$$L_{ij} = \frac{k_{ij}}{3}\sqrt{\frac{V_j}{V_i}}\left(\frac{\sin\varphi_{ij}}{E^{ij}}\sqrt{1-k_{ij}^2\cos^2\frac{\varphi_{ij}}{2}} + \frac{(1-k_{ij}^2)K^{ij}}{k_{ij}^2 E^{ij}}\right) - \left(1 + \frac{(1-2k_{ij}^2)}{3k_{ij}}\sqrt{\frac{V_j}{V_i}}\right), \qquad [C13]$$

$$M_{ij} = \frac{\left(1 + \frac{V_j}{V_i}\right)}{3E^{ij}}(1 - k_{ij}^2)^{1.5}\left(1 - \left(\frac{1 - k_{ij}^2 \cos^2 \frac{\varphi_{ij}}{2}}{1 - k_{ij}^2}\right)^{1,5}\right), \quad [C14]$$

$$N_{ij} = \frac{\varphi_{ij}}{E^{ij}} \frac{\left(1 - \frac{V_j \sin \varphi_{ij}}{V_i \varphi_{ij}}\right)}{\left(1 + \frac{V_j}{V_i}\right)}, \quad [C15]$$

$$O_{ij} = \frac{V_j \sin^2 \frac{\varphi_{ij}}{2}}{V_i E^{ij}}, \quad [C16]$$

$$P_{ij} = \left(1 - \frac{V_j}{V_i}\right)\frac{K^{ij}}{E^{ij}} + 1 + \frac{V_j}{V_i}, \quad [C17]$$

$$R_{ij} = \left(\frac{\delta_i \omega_i + \delta_i \omega_i}{V_i + V_j}\right), \quad [C18]$$

$$T_{ij} = \frac{2\sqrt{1 - k_{ij}^2}}{E^{ij}}\left(1 + \frac{V_j}{V_i}\right)\left(1 - \sqrt{\frac{1 - k_{ij}^2 \cos^2 \frac{\varphi_{ij}}{2}}{1 - k_{ij}^2}}\right), \quad [C19]$$

$$Q_{ij} = \frac{\varphi_{ij}}{E^{ij}}, \quad [C20]$$

where

$$V_i = \sqrt{u_{si}^2 + v_{si}^2}, \quad K^{ij} = \int_0^{\varphi_{ij}} \frac{\varphi}{\sqrt{1 - k_{ij}^2 \cos^2 \frac{\varphi}{2}}}, \quad E^{ij} = \int_0^{\varphi_{ij}} \sqrt{1 - k_{ij}^2 \cos^2 \frac{\varphi}{2}}\, d\varphi$$

and

$$k_{ij}^2 = \frac{4V_i V_j}{(V_i + V_j)^2}$$

are the total velocity of the dispersed phase, incomplete elliptic integrals of the first and second type and modulus of these integrals, respectively.

At asymptotic approximation for small angles $\varphi \ll 1$ the formulae [C6]–[C20] transform into the following expressions:

$$A_{ij} = \sqrt{1 - k_{ij}^2 + \frac{k_{ij}^2 \varphi_{ij}^2}{4}}, \quad [C21]$$

$$B_{ij} = \frac{k_{ij}^2 \varphi_{ij}\left(1 - \frac{V_j}{V_i} + \frac{V_j \varphi_{ij}^2}{4V_i}\right)}{2A_{ij}}, \quad [C22]$$

$$C_{ij} = \frac{k_{ij}^2}{2} \frac{V_j \varphi_{ij}^2}{V_i A_{ij}}, \quad [C23]$$

$$D_{ij} = 1 - \frac{V_j \varphi_{ij}^2}{3 V_i A_{ij}^2}, \quad [C24]$$

$$F_{ij} = -\left(1 + \frac{V_j}{V_i}\right)\left[1 - \frac{V_j}{V_i} + \frac{1}{3}\left(1 + \frac{V_j}{V_i}\right)(1 - k_{ij}^2 + A_{ij}\sqrt{1 - k_{ij}^2} + A_{ij}^2)\right] \frac{k_{ij}^2 \varphi_{ij}}{4 A_{ij}^2}, \quad [C25]$$

$$G_{ij} = \frac{\varphi_{ij}^2}{4 A_{ij}^3} \frac{V_j}{V_i}, \quad [C26]$$

$$H_{ij} = \frac{V_j \varphi_{ij}}{2 V_i A_{ij}} \left[1 + \frac{1}{A_{ij}^2} \left[\left[\frac{1 - \frac{V_j}{V_i}}{1 + \frac{V_j}{V_i}} \right] \right] \right], \quad [C27]$$

$$L_{ij} = k_{ij} \sqrt{\frac{V_j}{V_i}} \left(1 - \frac{\varphi_{ij}^2}{12 A_{ij}^2}\right), \quad [C28]$$

$$M_{ij} = -\left(1 + \frac{V_j}{V_i}\right) \frac{k_{ij}^2 \varphi_{ij}}{4}, \quad [C29]$$

$$N_{ij} = \frac{\left(1 - \frac{V_j}{V_i} + \frac{V_j \varphi_{ij}^2}{2 V_i}\right)}{2\left(1 + \frac{V_j}{V_i}\right) A_{ij}}, \quad [C30]$$

$$O_{ij} = \frac{V_j \varphi_{ij}}{2 V_i A_{ij}}, \quad [C31]$$

$$P_{ij} = 1 + \frac{V_j}{V_i} + \frac{1}{A_{ij}^2}\left(1 - \frac{V_j}{V_i}\right), \quad [C32]$$

$$T_{ij} = -\frac{k_{ij}^2 \varphi_{ij}}{2 A_{ij}^2}\left(1 + \frac{V_j}{V_i}\right), \quad [C33]$$

$$Q_{ij} = \frac{1}{A_{ij}}. \quad [C34]$$